1968

A study of joint conductance as a function of pressure between two thick walled concentric steel cylinders

Roger Harold Stoudt
Lehigh University

A STUDY OF JOINT CONDUCTANCE AS A FUNCTION OF PRESSURE BETWEEN TWO THICK WALLED CONCENTRIC STEEL CYLINDERS

by

Roger Harold Stoudt

A THESIS

Presented to the Graduate Faculty

of Lehigh University

in Candidacy for the Degree of

Master of Science

in

Mechanical Engineering

Lehigh University

1968

CERTIFICATE OF APPROVAL

This thesis is accepted and approved in partial fulfillment of the requirements for the degree of Master of Science.

September 16, 1968
Date

Robert A Lucas
Professor in Charge

Fabian F. Peer
Head of the Department

ACKNOWLEDGEMENTS

I wish to express my thanks to Robert Lucas, Ph.D., who supervised my work and provided invaluable guidance. His genuine interest and deep concern are very much appreciated.

I would also like to thank my wife, Joanne. Her patience, understanding, and ability to take data were valuable contributions to this thesis.

TABLE OF CONTENTS

LIST OF FIGURES

LIST OF TABLES

ABSTRACT

The following paper investigates the effect which pressure has on the joint conductance between two concentric, thick walled, low carbon steel cylinders in direct contact. Also, the transient response of the joint conductance and the interface pressure was noted for various heat fluxes.

The contact surfaces of the steel cylinders were lathe finished and had a surface roughness of approximately 120 micro-inches, rms. The hardness of both cylinders was measured and found to be 64 on the Rockwell E scale. The properties of the steel used were the published values for low carbon steel, namely, 26 BTU/-hr-ft-^{o}F for the thermal conductivity, 6.4 x 10^{-6} in/-in-^{o}F for the coefficient of thermal expansion, and .26 for Poisson's ratio.

The interface pressure varied between 3 and 6581 psi. Mean interface temperature varied between 164 and 276 ^{o}F. Heat flows of 1970 BTU/hr to 4130 BTU/hr, as they affected interface pressure, produced temperature drops across the interface of from less than 2 ^{o}F to as much as 60 ^{o}F. Joint conductances between 100 and 2050 BTU/hr-ft^{2}-^{o}F were recorded. Plots were made of conductance versus pressure and also conductance and

pressure versus time as obtained in the transient cases. These were compared to some published data of joint conductance as a function of pressure between two plane steel surfaces.

I. INTRODUCTION

Theoretically, any time two similar or dissimilar materials form a joint, heat flow across the joint from one material to the other is in no way impeded by the joint; and the surfaces forming the joint are at the same temperature. In reality this is not the case. The joint does impede heat flow and there is a temperature drop across the joint. In order to handle heat transfer problems involving joints, a method is used which is similar to that used in boundary layer problems. That is, heat flow across the joint is set equal to the temperature drop across the joint multiplied by the joint area multiplied by a quantity known as the joint conductance, the inverse of which is known as the thermal resistance. The joint conductance is a measure of the restriction placed on the heat flow by the joint. It is dependent upon such joint properties as pressure, roughness, temperature, orientation of the surfaces forming the joint, and flatness of the surfaces.

The problem of predicting joint conductance is a relatively new one. However, there has been a fair amount of investigation done in this area [1][1]. Generally, the method of approach is an experimental one.

---

1. Numbers in brackets designate references at the end of this thesis.

This is evidenced by the early works of W. B. Kouwenhoven and J. H. Potter [2], who explored the effects of pressure, temperature, and surface roughness on the thermal resistance of a steel-to-steel joint and found that the temperature level has a very small effect on thermal resistance. Another early work was that of A. W. Brunot and Florence F. Buckland [3], who obtained the thermal resistance of laminated and machined steel joints as a function of pressure. The investigation of N. D. Weills and E. A. Ryder [4] studied the thermal conductance between two metal surfaces as a function of temperature, pressure, and surface finish, a notable discovery being that different assemblies of the same joint produced different joint conductances at a particular pressure. Some recent experimental investigations are those of E. Fried [5], who looked at joint conductance in a vacuum as a function of pressure, and Martin E. Barzelay, Kin Nee Tong, and George Holloway [6], who obtained joint conductances between aluminum alloy and stainless steel blocks.

There have also been analytical approaches to the problem of joint conductance. Merril L. Minges [7] reviews the analytical approaches as well as the experimental approaches. Another similar endeavor is that of T. Nejat Veziroglu [8], who correlates experimental

results of the aforementioned authors and more.

In this investigation the experimental approach is used to determine the joint conductance. Nothing is unique about the material used or the results desired. What is unique is the interface geometry investigated. The experimenters mentioned previously were only concerned with determining the joint conductance between two plane surfaces, chiefly as a function of interface pressure. In this paper the joint conductance between two cylindrical surfaces as a function of interface pressure is studied. The transient behavior of the joint conductance due to the coupling of interface pressure and relative cylinder expansion is also considered.

The surface geometry chosen for investigation is typical of the type which is found in many industrial applications, such as heat exchanger and nuclear reactor design. Specifically, heat exchanger builders have historically been bothered with leakage around the rolled joints between the exchanger tubes and end plates. To more fully explain the factors which cause these leaks requires a knowledge of the operating thermal stresses at the connections. This in turn requires a knowledge of the temperature distributions which are partially dependent upon the joint conductance. During start up these conditions are generally more severe, and a know-

ledge of the transient behavior of the joint conductance would be useful.

II. ANALYTICAL CONSIDERATIONS

The theory involved in determining the conductance across a joint is straight forward, needs little explanation, and may be briefly summarized as follows:

The heat flow across the joint is given by[2]

$$\dot{q} = kA_j(dT/dr)_j \qquad (2\text{-}1)$$

where k is the thermal conductivity (a known value), A_j is the joint area, and $(dT/dr)_j$ is the temperature gradient at the joint. The heat flow can also be said to be

$$\dot{q} = hA_j(\Delta T)_j \qquad (2\text{-}2)$$

where $(\Delta T)_j$ is the temperature drop across the joint and h is the joint conductance. Equating these two expressions, we have

$$kA_j(dT/dr)_j = hA_j(\Delta T)_j \qquad (2\text{-}3)$$

And solving for h,

$$h = k(dT/dr)_j/(\Delta T)_j \qquad (2\text{-}4)$$

Therefore, by knowing the heat flow through the joint, i.e. - by knowing $(dT/dr)_j$, and by knowing the temper-

---

2. The variables occurring in the equations found in this paper are identified in Appendix A.

ature drop across the joint, the joint conductance can be calculated.

To establish the interface pressure, the technique of superposition of radial deformations is used. It is necessary to know the deformation of the inside radius of the outer cylinder and the outside radius of the inner cylinder. The standard thick walled cylinder analysis is employed as found in the text by Joseph H. Faupel [9].

The deformation of the inside radius, b_o, of the outer cylinder due to a pressure, p_o, on the outside surface is

$$- \frac{p_o b_o}{E_o} \left[\frac{2c^2}{c^2 - b_o^2} \right] \tag{2-5}$$

where the (-) sign indicates a contraction. A similar expression for the outside radius, b_i, due to a pressure, p_i, on the inside surface of the inner cylinder is

$$+ \frac{p_i b_i}{E_i} \left[\frac{2a^2}{b_i^2 - a^2} \right] \tag{2-6}$$

where the (+) sign indicates an expansion.

The deformation of the inside radius of the outer cylinder caused by the interface pressure, p_f, is

$$+ \frac{p_f b_o}{E_o}\left[\frac{c^2+b_o^2}{c^2-b_o^2}+\nu_o\right] \qquad (2\text{-}7)$$

And similarly for the inner cylinder, the expression is

$$- \frac{p_f b_i}{E_i}\left[\frac{b_i^2+a^2}{b_i^2-a^2}-\nu_i\right] \qquad (2\text{-}8)$$

The assumed temperature distribution, T, also produces deformations. These are, for the inside radius of the outer cylinder

$$+ \frac{2\alpha_o}{c^2-b_o^2}\int_{b_o}^{c} Tr\,dr \qquad (2\text{-}9)$$

and for the outer radius of the inner cylinder

$$+ \frac{2\alpha_i}{c^2-b_i^2}\int_{a}^{b_i} Tr\,dr \qquad (2\text{-}10)$$

If there is a compressive load, L, applied to the inner cylinder, the change in the outside radius is

$$+ \frac{2L\nu_i b_i}{E_i} \qquad (2\text{-}11)$$

Since the radii must match at the interface, the resulting equation is

$$b_i + \frac{p_i b_i}{E_i}\left[\frac{2a^2}{b_i^2-a^2}\right] - \frac{p_f b_i}{E_i}\left[\frac{b_i^2+a^2}{b_i^2-a^2}-\nu_i\right] +$$

$$+ \frac{2\alpha_i}{c^2 - b_i^2} \int_a^{b_i} Tr\,dr + \frac{2L\nu_i b_i}{E_i} = b_o - \frac{p_o b_o}{E_o}\left[\frac{2c^2}{c^2 - b_o^2}\right]$$

$$+ \frac{p_f b_o}{E_o}\left[\frac{c^2 + b_o^2}{c^2 - b_o^2} + \nu_o\right] + \frac{2\alpha_o}{c^2 - b_o^2} \int_{b_o}^{c} Tr\,dr \qquad (2\text{-}12)$$

This equation can be solved for p_f. Hence, for a given temperature profile, the corresponding interface pressure can be calculated.

An alternative method is that of directly measuring the hoop or circumferential stress, σ_H, on the inside cylindrical surface of the inner cylinder. This stress could then be related to the interface pressure by the equation

$$\sigma_H = \left[\frac{E_i \alpha_i}{1 - \nu_i}\right]\left[\frac{1}{a^2}\right]\left[\frac{2a^2}{b_i^2 - a^2} \int_a^{b_i} Tr\,dr - Ta^2\right]$$

$$+ \frac{a^2 p_i - b_i^2 p_f}{b_i^2 - a^2} + \frac{b_i (p_i - p_f)}{b_i^2 - a^2} \qquad (2\text{-}13)$$

Therefore, knowing the hoop stress and knowing the temperature profile in the inner cylinder allows the corresponding interface pressure to be calculated.

III. DESIGN OF THE EXPERIMENT

3.1 Preliminary Considerations

To develop a sufficient temperature gradient without high heat input in the experimental apparatus, it was decided to use two concentric cylinders made of low carbon steel, a common material having a moderate thermal conductivity.

In order to determine the joint conductance, a heat flux across the interface was necessary. This was provided by a Chromalox, 1500 watt heater band which was clamped around the outer cylinder. Cooling was also needed and this was done by water cooling the inside cylinder.

The cylinders also had to be thick (4 inches was decided upon) so that the interface pressure would be relatively constant and the end effects could be neglected. (See figure 1 for a preliminary plan.)

3.2 Thermocouple Technique

As explained in the introduction, the joint or interface conductance can be determined if the temperature gradient at the interface is known, and if the temperature drop across the interface is known. To determine these two quantities, four thermocouples were used on each side of the joint. The number four was decided upon because it allowed a reasonably sized apparatus to be used while still providing enough data points to establish a reliable temperature profile. The thermocouple spacing used appears in figure 2. Thermocouples 4 and 5 were located as close together as possible to eliminate error in the calculation of temperature drop across the joint. Note that the thermocouples do not lie on the same radius. This was done to prevent one thermocouple from disrupting the temperature profile near another.

The thermocouples selected for use were Conax thermocouples made of copper and constantan wires passing through a magnesium oxide insulation contained in a 3 inch long stainless steel sheath. The wires were welded to the sheath tip for good thermal response and the sheath was .040 inches in diameter to assure exact thermocouple location. The accuracy of the thermocouples was certified by the manufacturer to be $\pm 1.2\ ^{o}F$ in the

temperature range operated in.

The installation of the thermocouples was accomplished by drilling .062 inch holes, 2 inches in depth, in the cylinder sides. These holes were then enlarged to a depth of 1/2 inch and threaded to receive a Conax Packing Gland which held the thermocouple firmly in place against the bottom of the drilled hole, assuring good tip contact. Other techniques have been used to assure tip contact such as dental cement and copper filings, but it was felt that this method provided better point contact. (See figure 3 for a picture of the thermocouple installation.)

3.3 Interface Pressure

In order to study joint conductance as a function of interface pressure, it is necessary to be able to vary the interface pressure. In this investigation two techniques were employed.

The first of the techniques involved varying the heat input to the apparatus. Any heat input at all imposes a radial temperature gradient in the cylinder. This means that as the cylinders expand, they will not expand uniformly. Since the outside cylinder in this investigation is being heated, it will expand more than the inside cylinder which is being cooled. Thus, providing a pressure gradient existed before heating, there will be a decrease in the interface pressure.

Obviously, the above condition mandates that the two cylinders be shrink fitted together in order to provide an initial pressure and maintain contact. The initial pressure also had to be low enough to permit the heater output (limited to 1500 watts) to expand the cylinder differentially and operate in the interface pressure region (0 - 4000 psi) which would probably influence joint conductance the most. The procedure to determine the interference of the cylinder diameters is as follows:

First, it was decided that at maximum heater in-

put, the interface pressure should be zero. So, knowing the heat input and assuming a temperature at the inside surface of the inner cylinder, it was possible to get a theoretical temperature distribution of the form

$$T = T_i - \left[\frac{(T_i - T_o)}{\ln (c/a)}\right] \ln (r/a) \qquad (3.3\text{-}1)$$

Next, the general equation (2-12), which relates interface pressure and temperature profiles, was simplified. Both cylinders were of the same material. Therefore,

$$E_o = E_i \quad \nu_o = \nu_i \quad \alpha_o = \alpha_i \qquad (3.3\text{-}2)$$

Because an interface pressure of zero is desired for the assumed temperature distribution, both terms involving p_f are zero. The resulting expression is

$$b_i + \frac{p_i b_i}{E}\left[\frac{2a^2}{b_i^2 - a^2}\right] + \frac{2\alpha}{c^2 - b_i^2}\int_a^{b_i} Tr\, dr =$$

$$b_o - \frac{p_o b_o}{E}\left[\frac{2c^2}{c^2 - b_o^2}\right] + \frac{2\alpha}{c^2 - b_o^2}\int_{b_o}^{c} Tr\, dr \qquad (3.3\text{-}3)$$

All the quantities are known in this expression except b_i and b_o. The quantity b_o was set equal to 3.25 inches, the nominal interface radius, and the equation was then solved for b_i using a computer program. This resulted

in a b_o of 3.2516 inches and a diametrical interference of .0032 inch.

The second method of varying the interface pressure was to make use of the Poisson's effect in materials. That is, by compressing the inner cylinder in the axial direction, the cylinder would grow in the radial direction, thereby increasing the interface pressure. Using a 60,000 pound testing machine, a 300 psi pressure increase could be realized.

To actually determine the interface pressure, two approaches were used. One was to use equation (2-12). Knowing the temperature profiles in both cylinders from thermocouple measurments, the corresponding interface pressure could be calculated. An alternative to this procedure involved the installation of strain gages on the inside cylindrical surface of the inner cylinder. One gage was installed in an axial direction and another in a circumferential direction. To correct for any temperature effects at this surface, either the gage in the axial direction was used as a dummy gage or a precision resistor was employed, the difference in these two techniques being negligible. To relate hoop or circumferential stress obtained in this way to the interface pressure, the appropriate equation is (2-13).

3.4 Other Considerations

In arriving at the apparatus dimensions, all of the items previously discussed had to be considered simultaneously. The necessary access space for installation of strain gages on the inner cylinder fixed the inside radius of the inner cylinder. Also, the thermocouple spacing, added to the fixed inside radius of the inner cylinder, dictated the nominal interface radius as well as the outside radius of the outer cylinder. (See figure 4 for dimensions.)

In order to squeeze the inside cylinder axially to increase the interface pressure, two compression fixtures were designed as shown in figure 5. These fixtures transmitted load through Pyroceram spacers which, having a low thermal conductivity as well as a high compressive strength, were used to prevent axial heat flow from the inner cylinder. The fixtures also served as inlet and outlet headers for the cooling water, utilizing O-ring seals between the fixtures and the inner cylinder. Provision was made for thermometer installation to check cooling water temperatures.

Assembly of the two concentric cylinders was accomplished by heating the outside cylinder to 200 ^{o}F and cooling the inside cylinder to -100 ^{o}F. This permitted the two cylinders to slip easily together. It

should also be mentioned that before assembly, the surfaces forming the interface were cleaned with a wire brush, fine emery paper, and carbon tetrachloride to remove oxide and any oil or grease which might be present. The surface roughness of the contact surfaces was checked and found to be 120 micro inches, rms. The hardness was also measured and found to be 64 on the Rockwell E scale.

After assembly the joint was sealed with silicone rubber to prevent entrance of foreign matter and/or rusting. The compression fixtures were attached next and the apparatus placed in a Baldwin 60,000 pound testing machine. Polyurethane foam was used to insulate the outer cylinder to prevent axial heat flow. Fiberglass building insulation was used around the heater to minimize heat losses to the atmosphere. The air gap between the inner cylinder and the compression fixtures plus the Pyroceram spacers minimized axial heat flow there. Incoming cooling water was passed through a pressure regulator and monitored with a pressure gage. The complete assembly is shown in figure 6. A list of equipment used for measurement purposes can be found in appendix B.

IV. CONDUCTANCE OF TESTS

Twelve tests were run utilizing different heat inputs which ranged from 1970 to 4130 BTU/hr. Thermocouple readings were taken every 20 minutes until the apparatus reached steady state. Strains in the circumferential direction were also noted at these intervals. Two tests were conducted utilizing two fixed heat inputs with axial loadings of 20,000, 40,000, and 55,000 pounds. The condensed data from these tests appears in appendix C.

Next, a computer program employing the method of least squares was used to fit a curve to each of data. A second order fit was used. The coordinates axes were placed on the interface so that the temperatures in each cylinder appeared as a function of the form

$$T = A + Bx + Cx^2 \qquad (4\text{-}1)$$

where x is the distance from the interface and A, B, and C are the curve fit coefficients. The temperature on each contact surface was obtained by substituting 0 for x. The temperature drop across the joint was obtained by subtracting one surface temperature from the other. To determine the temperature gradient at the joint, the equation for T was differentiated with respect to x and then 0 substituted for x. Subsequently, the

joint conductance could be determined with equation (2-4). Then entering equation (2-12) with the computer curve fit equations, translated from x to r coordinates, the interface pressure was determined. This was checked by using equation (2-13). In all these tests the mass flow rate of the cooling water was maintained between 600 and 636 lb_m/hr, which fixed the water pressure on the inner cylinder at approximately 16 psi. The mean water temperature was about 66 ^oF.

V. INTRODUCTION OF RESULTS

Using the procedure descrived in the last chapter, the data appearing in Appendix C was reduced and appears in Tables 1 thru 14. The two quantities, $(dT/dr)_j$ and $(\Delta T)_j$, which were gotten directly from the curve fit program appear in these tables along with the joint conductance, h, and the interface pressure, p_f, as a function of time for a given heat input. An exception to this are Tables 12 and 14 where $(dT/dr)_j$, $(\Delta T)_j$, the conductance, and the interface pressure are a function of compressive load on the inner cylinder, which was 0 in the other cases. In all the tables, the symbol (ss) denotes steady state values and an asterisk (*) indicates questionable values.

Figures 1 thru 6 need no explanation since these concern apparatus design and have been refered to previously.

Figure 7 is a plot of joint conductance, h, versus interface pressure, p_f, obtained from steady state data. The dotted lines on either side of the joint conductance curve represent the limits of experimental error.

A plot similar to Figure 7 is that of Figure 8, which shows joint conductance as a function of interface pressure obtained by plotting all data points. Again the dotted lines are the limits of experimental

error which appear in Figure 7.

Figures 9 thru 20 are the transient responses of joint conductance and interface pressure for a given heat input. Joint conductance also appears as a function of interface pressure.

Figure 21 is a plot of joint conductance versus interface pressure which was varied by an axial compressive load on the inner cylinder, keeping heat input constant. All points represent steady state data. Also, the appropriate portion of the curve in Figure 7 along with the limits of error appears in Figure 21 for comparison purposes.

VI. TABLES

TABLE 1

Calculated Data for Run Number 1

time (hrs:min)	$(dT/dr)_j$ (°F/in)	$(\Delta T)_j$ (°F)	h (BTU/hr-ft^2-°F)	p_f (psi)
0	—	—	—	—
:20	3.06	1.51	632	6581
:40	5.01	1.48	1055	6254
1:00	6.48	1.70	1190	6054
1:20	6.27	1.66	1180	6022
1:40	6.24	1.72	1140	5975
2:00	8.14	1.61	1580	5785
2:20	8.00	2.15	1160	5788
2:40	7.70	2.20	1090	5753
3:00	8.17	1.87	1365	5736
3:20	8.37	1.92	1360 (ss)	5739

heat input: 1970 BTU/hr

TABLE 2

Calculated Data for Run Number 2

time (hrs:min)	$(dT/dr)_j$ (°F/in)	$(\Delta T)_j$ (°F)	h (BTU/hr-ft^2-°F)	p_f (psi)
0	——	——	—	——
:20	4.34	2.08	651	6106
:40	7.24	2.61	866	5825
1:00	10.70	2.59	1288	5521
1:20	10.14	2.59	1223	5488
1:40	10.48	2.63	1242	5328
2:00	13.92	2.09	2080*	5120
2:20	13.51	3.14	1345	5033
2:40	13.93	2.93	1485	5026
3:00	14.01	3.08	1420	5026
3:20	14.29	3.07	1450 (ss)	4961

heat input: 2550 BTU/hr

TABLE 3

Calculated Data for Run Number 3

time (hrs:min)	$(dT/dr)_j$ (^oF/in)	$(\Delta T)_j$ (^oF)	h (BTU/hr-ft^2-^oF)	p_f (psi)
0	—	—	—	—
:20	5.18	2.74	590	5885
:40	8.75	2.42	1130	5687
1:00	10.32	2.48	1295	5325
1:20	11.09	3.45	1003	5103
1:40	11.68	4.03	905	4905
2:00	13.96	4.19	1040	4635
2:20	14.25	4.94	900	4664
2:40	14.25	5.00	890	4607
3:00	14.59	5.70	800	4540
3:20	15.16	5.83	810	4476
3:40	14.30	5.45	816 (ss)	4524

heat input: 2870 BTU/hr

TABLE 4

Calculated Data for Run Number 4

time (hrs:min)	$(dT/dr)_j$ (°F/in)	$(\Delta T)_j$ (°F)	h (BTU/hr-ft^2-°F)	p_f (psi)
0	——	——	——	——
:20	4.84	2.22	681	5935
:40	9.55	2.49	1195	5381
1:00	11.89	3.53	1050	4973
1:20	12.82	4.47	892	4842
1:40	12.81	5.77	693	4623
2:00	14.37	6.62	678	4386
2:20	15.06	7.03	668	4318
2:40	13.88	7.52	576	4350
3:00	14.70	7.61	603	4216
3:20	14.82	7.98	578	4274
3:40	15.60	7.47	650 (ss)	4268

heat input: 2930 BTU/hr

TABLE 5

Calculated Data for Run Number 5

time (hrs:min)	$(dT/dr)_j$ (°F/in)	$(\Delta T)_j$ (°F)	h (BTU/hr-ft^2-°F)	p_f (psi)
0	——	——	——	——
:22	6.27	1.94	1008	6000
:40	9.58	2.47	1210	5477
1:00	11.50	3.55	1012	4908
1:20	11.72	3.53	1035	4844
1:40	——	——	——	——
2:00	12.48	5.18	750	4638
2:20	14.81	5.78	796	4440
2:40	15.92	6.64	748	4351
3:00	15.36	6.83	703	4330
3:20	15.05	7.44	632	4214
3:40	14.68	7.16	638 (ss)	4289

Heat input: 3100 BTU/hr

TABLE 6

Calculated Data for Run Number 6

time (hrs:min)	$(dT/dr)_j$ (^oF/in)	$(\Delta T)_j$ (^oF)	h (BTU/hr-ft^2-^oF)	p_f (psi)
0	——	——	—	——
:20	4.18	2.46	540	5590
:40	10.38	2.91	1115	5141
1:00	12.28	3.51	1095	4856
1:20	13.95	1.82	2400*	4891
1:40	12.89	5.75	698	4528
2:00	15.26	6.56	726	4240
2:20	15.54	6.98	693	4299
2:40	15.45	7.13	677	4275
3:00	15.48	7.09	681	4265
3:21	15.86	7.39	670	4210
3:40	——	——	—	——
4:00	15.69	7.77	630 (ss)	4200

heat input: 3150 BTU/hr

TABLE 7

Calculated Data for Run Number 7

time (hrs:min)	$(dT/dr)_j$ (^oF/in)	$(\Delta T)_j$ (^oF)	h (BTU/hr-ft^2-^oF)	p_f (psi)
0	——	——	——	——
:21	5.19	2.81	577	5175
:40	11.28	2.88	1320	5065
1:00	13.65	3.68	1158	4726
1:20	12.38	4.86	795	4676
1:40	12.48	5.63	690	4592
2:00	15.31	7.66	623	4214
2:20	14.87	8.02	578	4183
2:40	15.43	9.13	528	4068
3:02	15.70	10.16	482	3948
3:22	15.78	10.05	489	3976
3:40	15.82	10.67	462	3900
4:00	16.16	11.68	433 (ss)	3802

heat input: 3270 BTU/hr

TABLE 8

Calculated Data for Run Number 8

time (hrs:min)	$(dT/dr)_j$ (°F/in)	$(\Delta T)_j$ (°F)	h (BTU/hr-ft^2-°F)	p_f (psi)
0	——	——	——	——
:20	5.42	2.57	657	5609
:40	9.83	2.69	1140	5225
1:00	13.35	3.73	1115	4764
1:20	12.55	5.50	713	4576
1:40	12.79	7.01	569	4391
2:00	15.33	8.91	537	4014
2:20	15.43	8.85	544	4030
2:40	15.14	9.85	480	3971
3:00	15.87	10.47	473	3897
3:20	15.74	12.90	381	3711
3:40	14.38	13.00	345	3801
4:00	15.75	14.24	344	3656
4:20	15.08	13.76	342 (ss)	3734

heat input: 3370 BTU/hr

TABLE 9

Calculated Data for Run Number 9

time (hrs:min)	$(dT/dr)_j$ (^oF/in)	$(\Delta T)_j$ (^oF)	h (BTU/hr-ft^2-^oF)	p_f (psi)
0	—	—	—	—
:20	5.73	1.94	922	5822
:40	10.05	2.01	1563	5013
1:00	16.81	2.53	2050	5055
1:20	11.39	1.75	2030	4669
1:40	12.57	3.93	998	4376
2:00	12.57	7.17	547	4100
2:20	16.44	7.02	731	3463
2:40	16.88	11.22	468	3177
3:00	16.44	23.36	219	3038
3:20	16.93	23.62	223	2914
3:40	17.16	21.29	251	2964
4:00	18.11	22.32	253	2824
4:20	—	—	—	—
4:40	19.12	23.27	256 (ss)	2709

heat input: 3560 BTU/hr

TABLE 10

Calculated Data for Run Number 10

time (hrs:min)	$(dT/dr)_j$ (°F/in)	$(\Delta T)_j$ (°F)	h (BTU/hr-ft^2-°F)	p_f (psi)
0	——	——	——	——
:20	4.72	3.17	464	5414
:40	11.34	2.92	1213	4971
1:00	13.83	4.97	868	4490
1:20	13.31	7.97	522	4225
1:40	13.71	11.37	377	3872
2:00	15.68	15.95	307	3426
2:20	16.86	18.75	280	3235
2:40	16.91	20.22	261	3100
3:00	17.73	20.34	272	3048
3:20	18.14	21.26	266	2939
3:40	18.93	22.38	264	2830
4:00	18.74	23.06	253	2772
4:20	19.02	24.40	243	2686
4:40	19.31	24.30	247 (ss)	2614
**	20.01	27.27	229 (ss)	2538

heat input: 3650 BTU/hr except for ** which is 3820 BTU/hr

TABLE 11

Calculated Data for Run Number 11

time (hrs:min)	$(dT/dr)_j$ (°F/in)	$(\Delta T)_j$ (°F)	h (BTU/hr-ft^2-°F)	p_f (psi)
0	——	——	——	——
:20	——	——	——	——
:40	12.24	4.48	852	4563
1:00	——	——	——	——
1:20	16.26	18.43	275	3145
1:40	——	——	——	——
2:00	18.42	28.89	199	2285
2:20	——	——	——	——
2:50	17.24	35.25	153	1858
3:00	——	——	——	——
3:20	17.78	38.84	143	1563
3:40	——	——	——	——
4:00	18.73	42.60	137	1326
4:20	——	——	——	——
4:40	19.65	44.88	136	1083
5:00	——	——	——	——
5:20	19.13	44.50	134 (ss)	1104

heat input: 4000 BTU/hr

TABLE 12

Calculated Data for Run Number 12

load, L (psi)	$(dT/dr)_j$ (^oF/in)	$(\Delta T)_j$ (^oF)	h (BTU/hr-ft^2-^oF)	p_f (psi)
20000	20.92	43.69	150 (ss)	1208
40000	21.41	43.74	153 (ss)	1288
55000	20.82	35.77	181 (ss)	1839

heat input: 4000 BTU/hr

TABLE 13

Calculated Data for Run Number 13

time (hrs:min)	$(dT/dr)_j$ (°F/in)	$(\Delta T)_j$ (°F)	h (BTU/hr-ft^2-°F)	p_f (psi)
0	——	——	——	——
:20	7.16	2.72	821	5336
:40	12.68	4.67	848	4482
1:00	15.29	11.64	412	3660
1:20	15.03	20.47	229	3039
1:40	18.48	26.86	214	2409
2:00	22.59	32.23	218	1855
2:20	24.33	37.24	204	1429
2:40	25.22	36.92	213	1502
3:00	25.64	38.62	207	1233
3:20	27.62	41.65	207	946
3:40	24.82	49.33	157	636
4:00	22.57	50.60	139	574
4:20	20.75	54.65	119	586
4:40	20.78	54.08	119	440
5:00	20.68	56.39	114	232
5:20	21.13	59.08	111	3
5:40	20.62	59.13	109 (ss)	6

heat input: 4130 BTU/hr

TABLE 14

Calculated Data for Run Number 14

load, L (psi)	$(dT/dr)_j$ ($^{\circ}F$/in)	$(\Delta T)_j$ ($^{\circ}F$)	h (BTU/hr-ft^2-$^{\circ}F$)	p_f (psi)
20000	19.18	59.89	100 (ss)	99
40000	23.65	60.03	123 (ss)	16
55000	22.13	59.08	116 (ss)	13

heat input: 4130 BTU/hr

VII. FIGURES

FIGURE 1

Preliminary Test Specimen Configuration

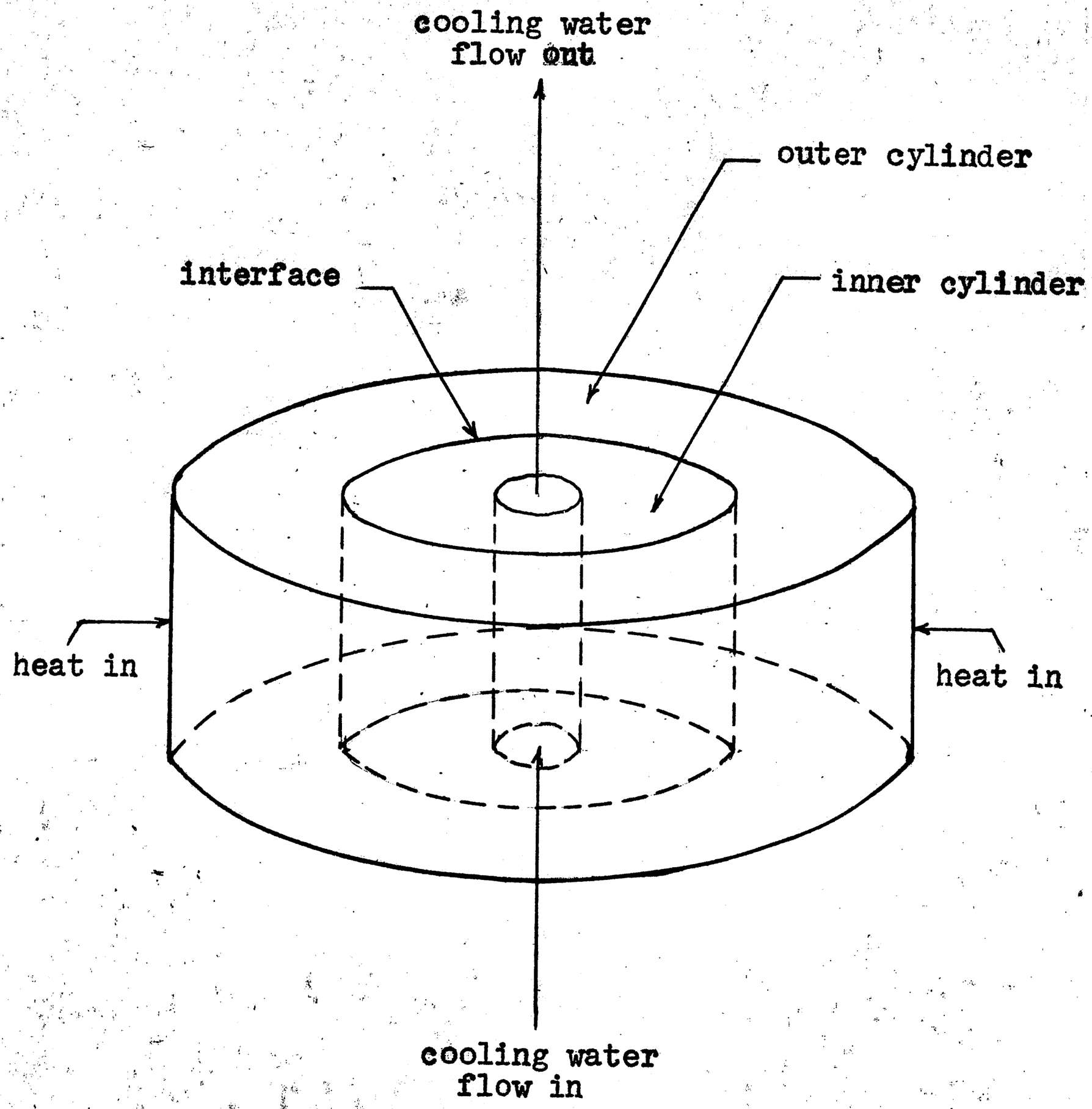

FIGURE 2

Thermocouple Locations

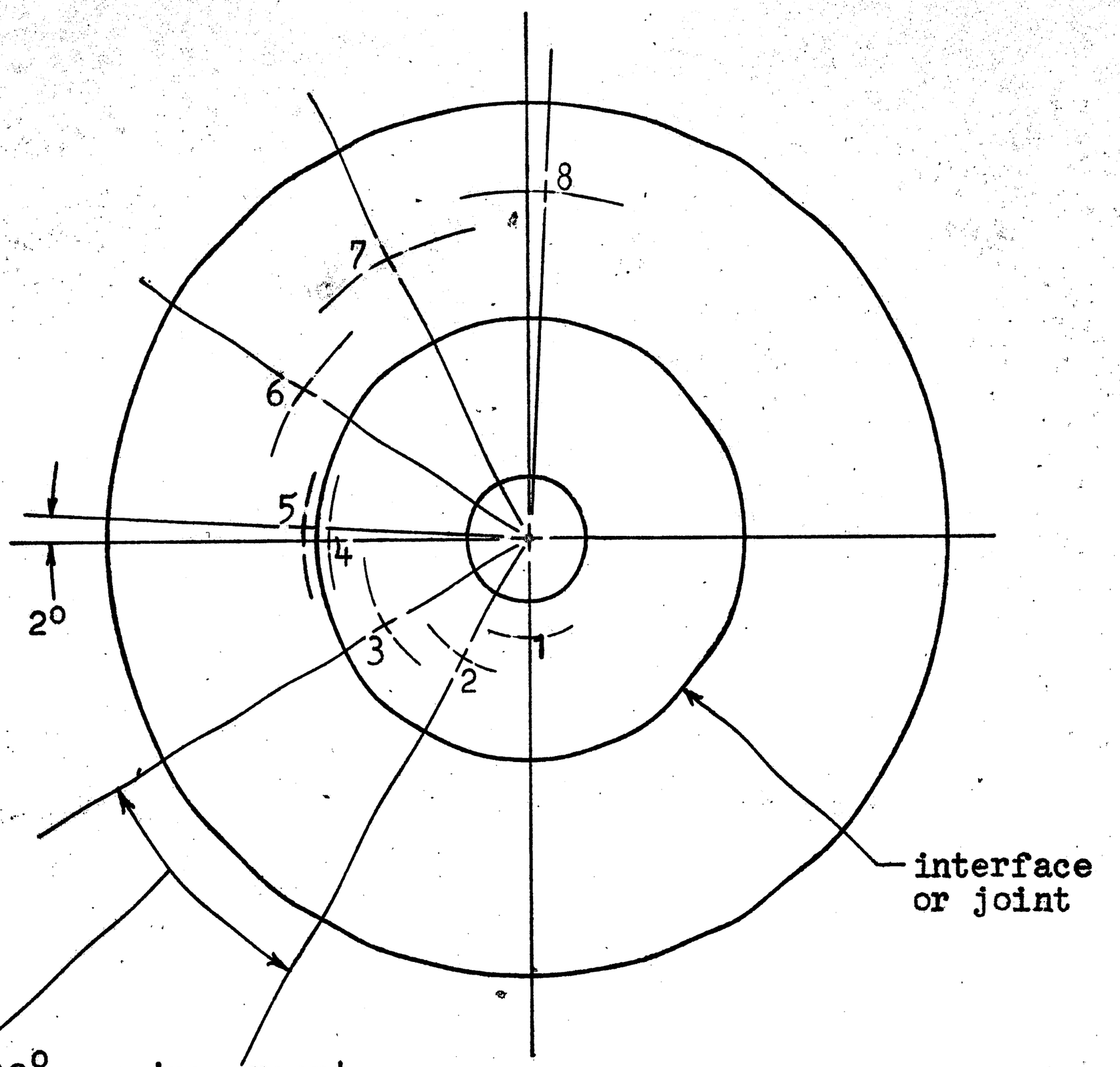

thermocouple	distance from joint (ins)
1	1.837
2	1.372
3	.837
4	.050
5	.050
6	.650
7	1.260
8	1.695

FIGURE 3

Thermocouple Installation

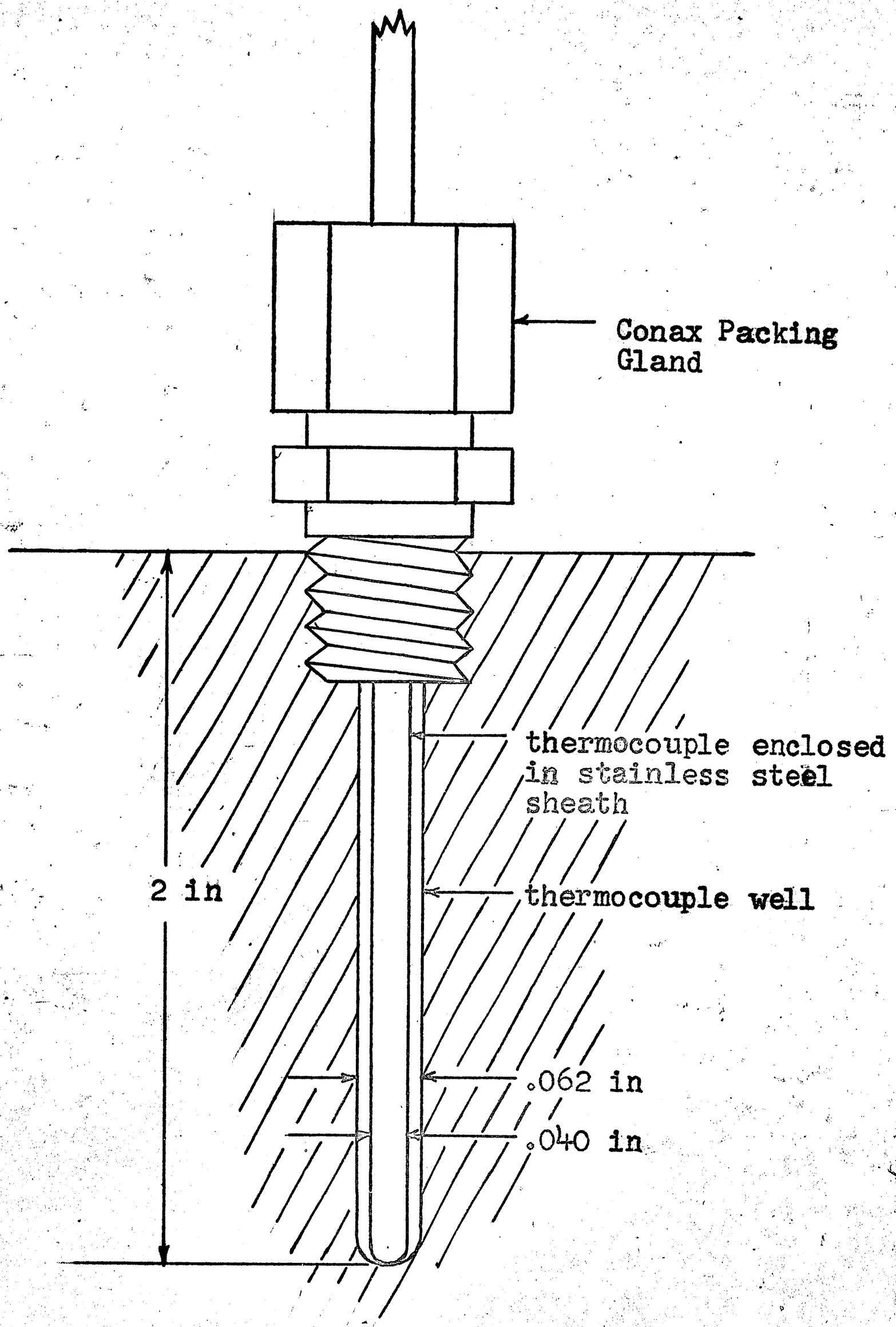

FIGURE 4

Final Test Specimen Configuration

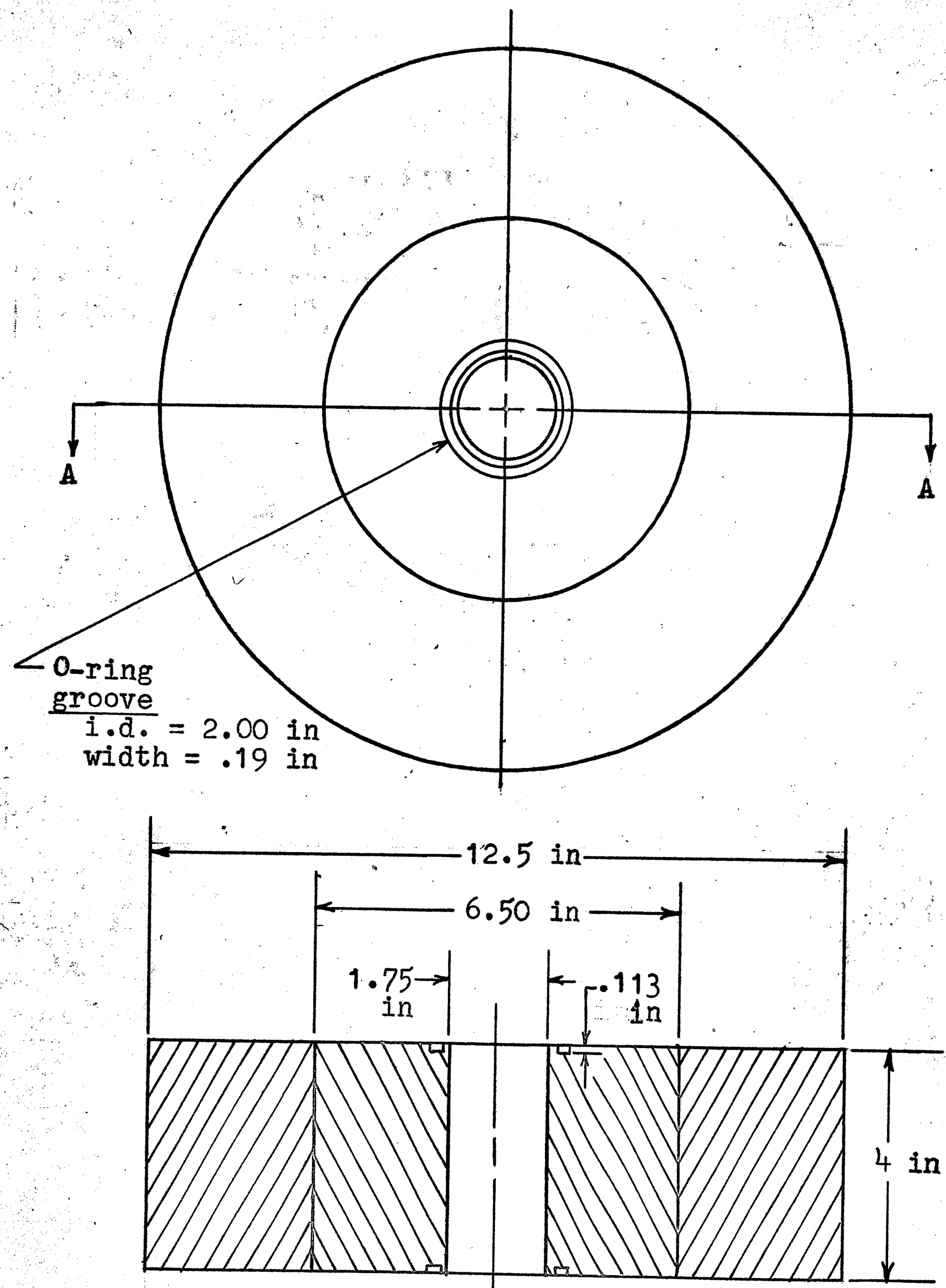

Section AA

FIGURE 5

Compression and Cooling Fixture Design

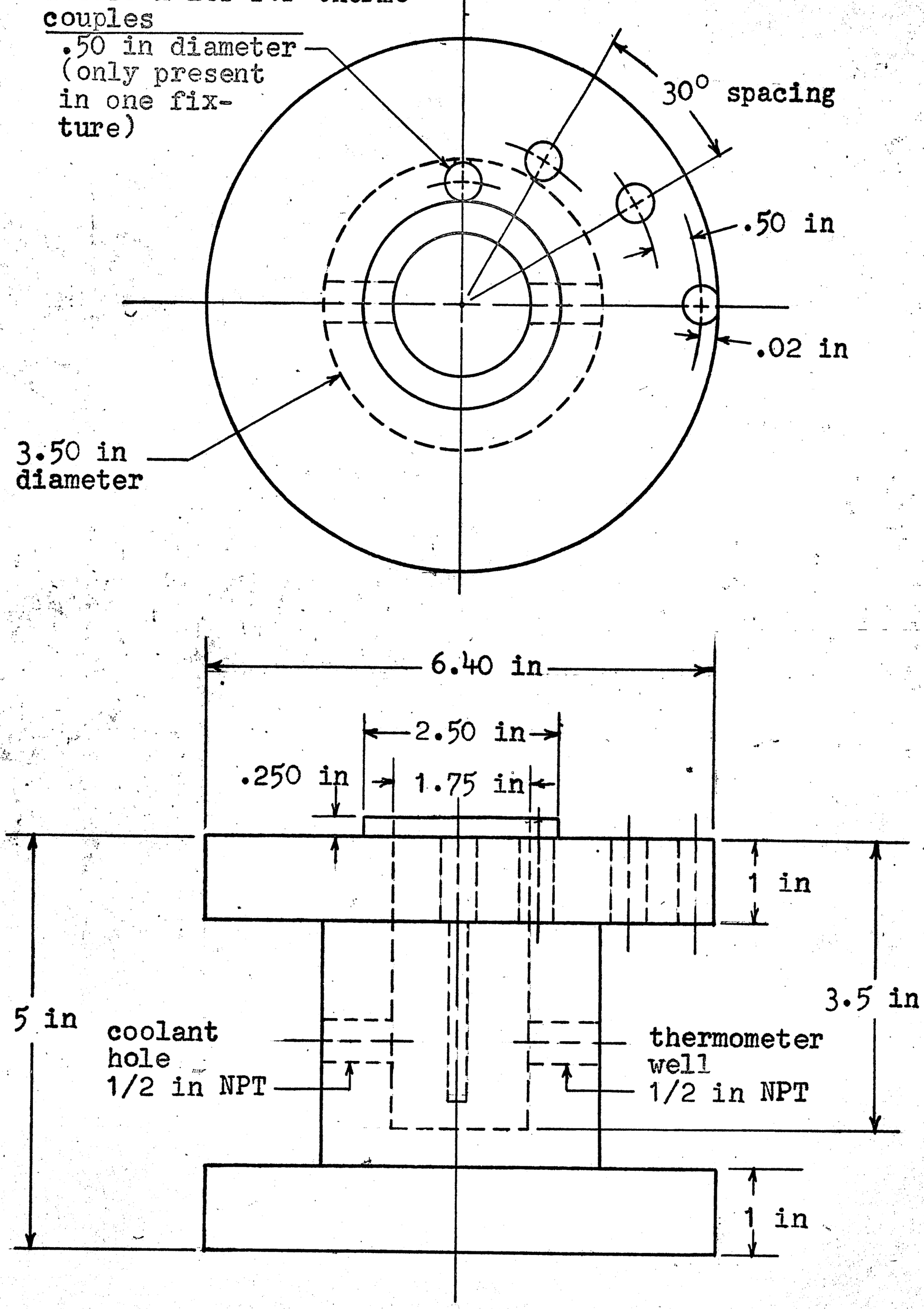

FIGURE 6

Assembly of Test Specimen and Test Apparatus

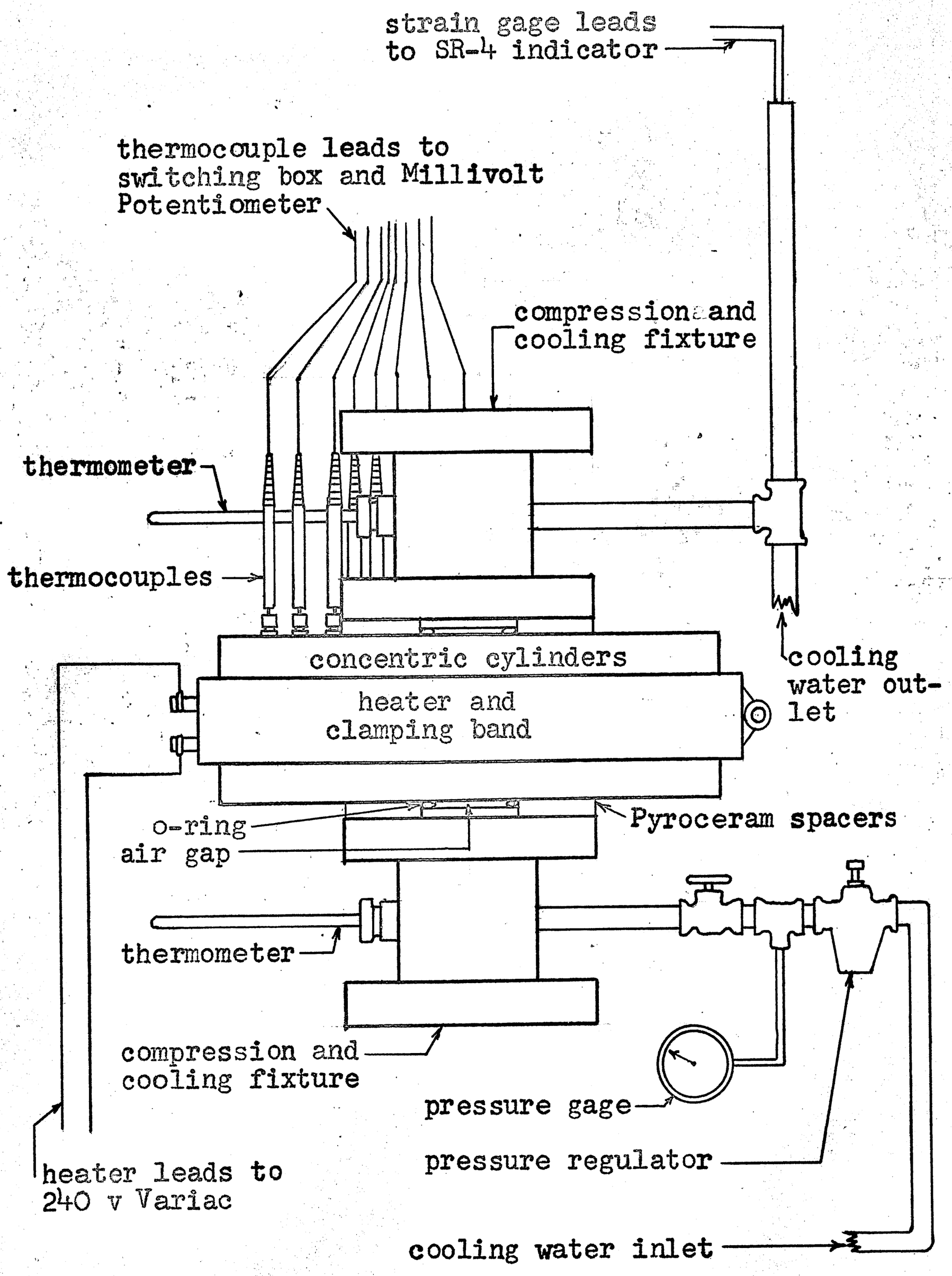

FIGURE 7

Conductance versus Pressure Utilizing
Steady State Data Points

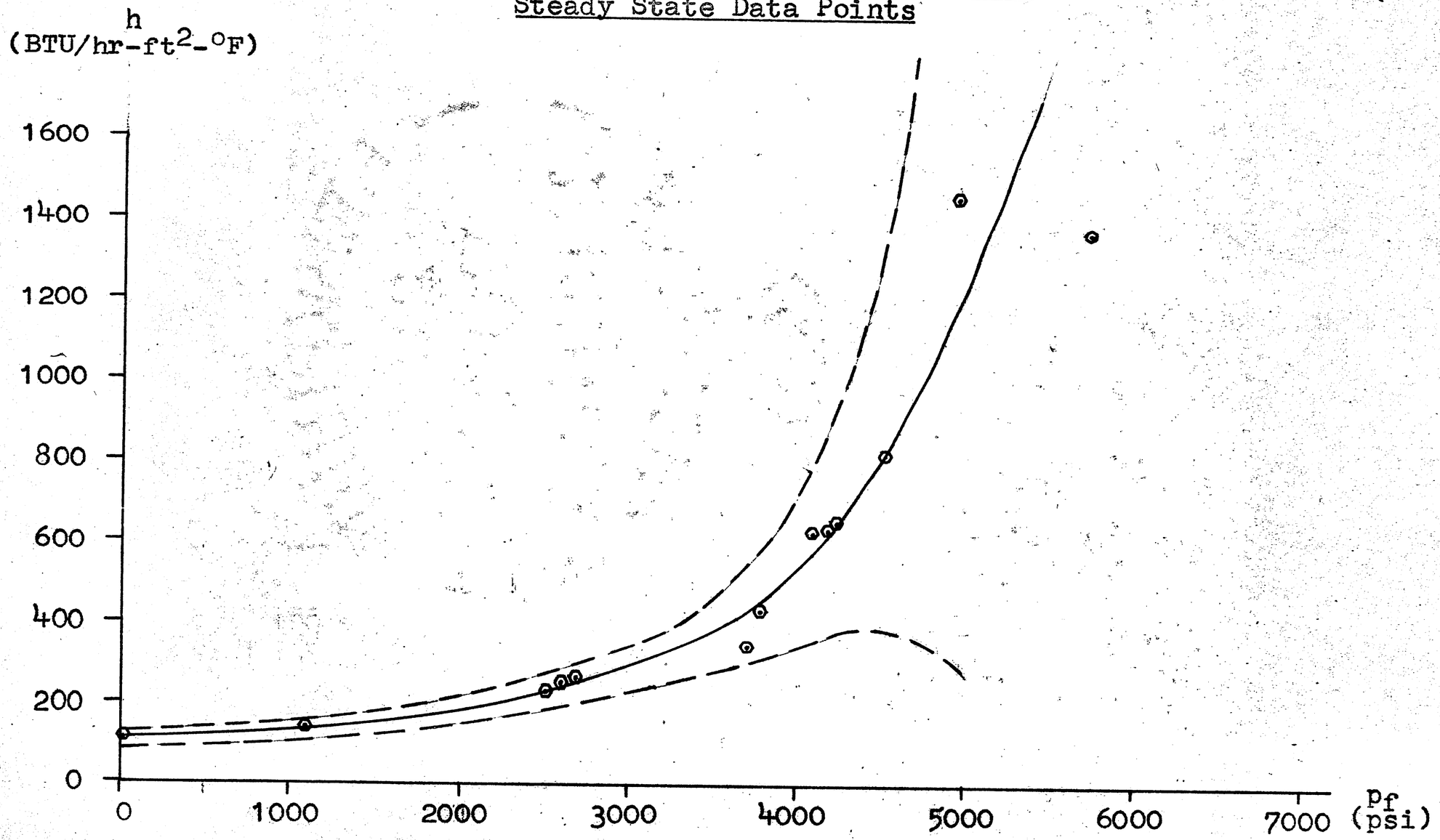

FIGURE 8

Conductance versus Pressure Utilizing
All Data Points

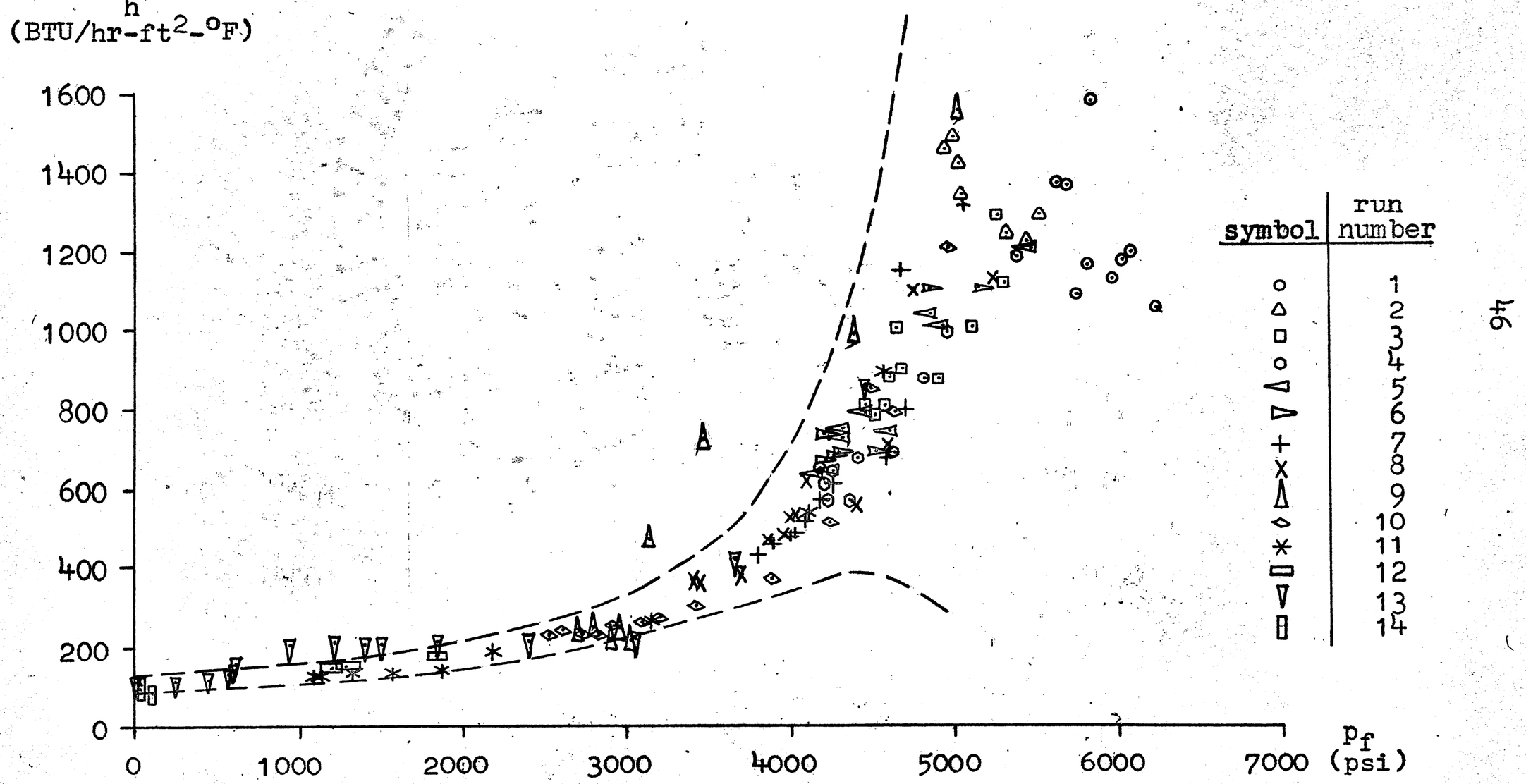

FIGURE 9

Transient Response of Conductance and Pressure and Conductance versus Pressure - Run Number 1

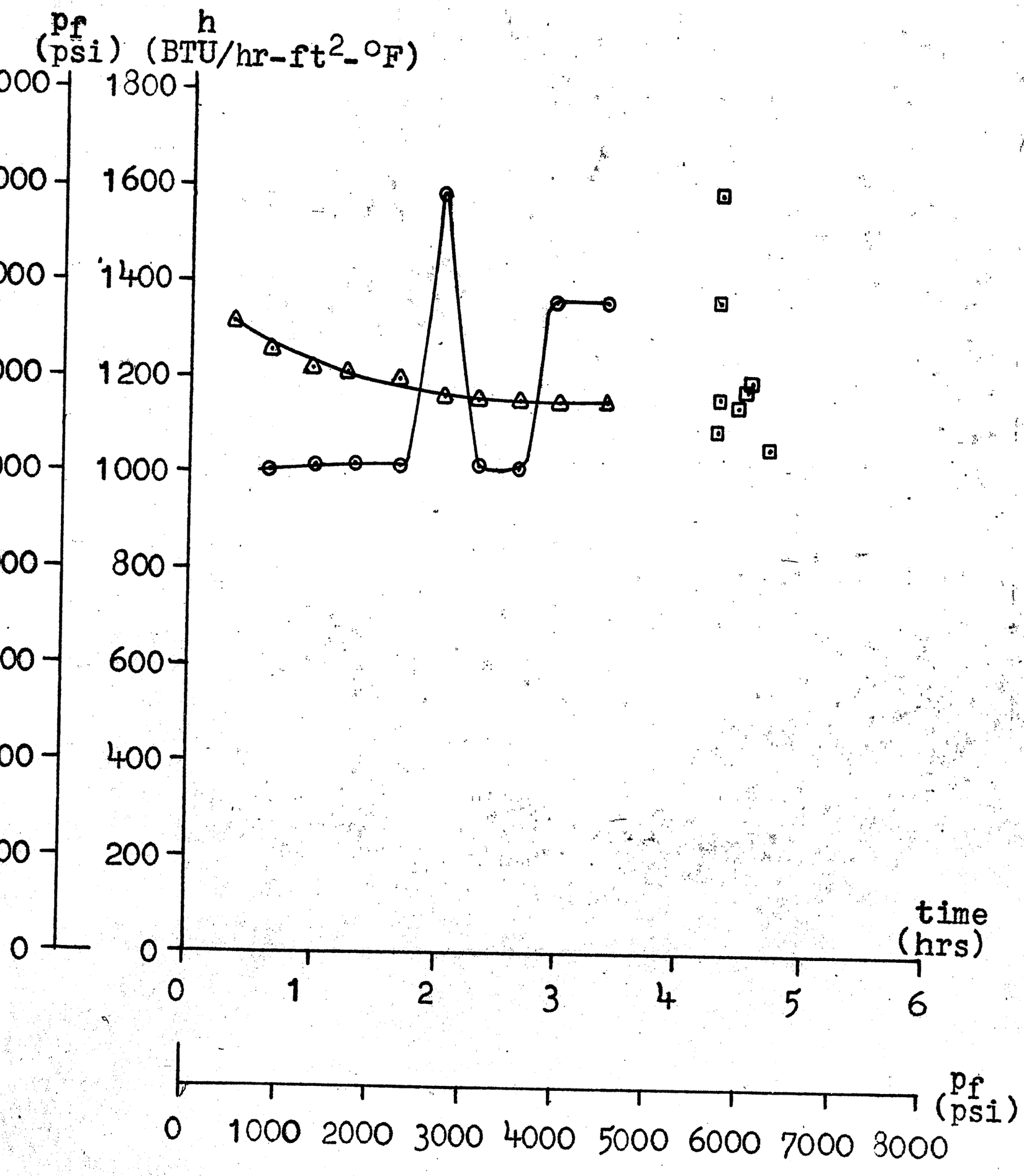

FIGURE 10

Transient Response of Conductance and Pressure and Conductance versus Pressure - Run Number 2

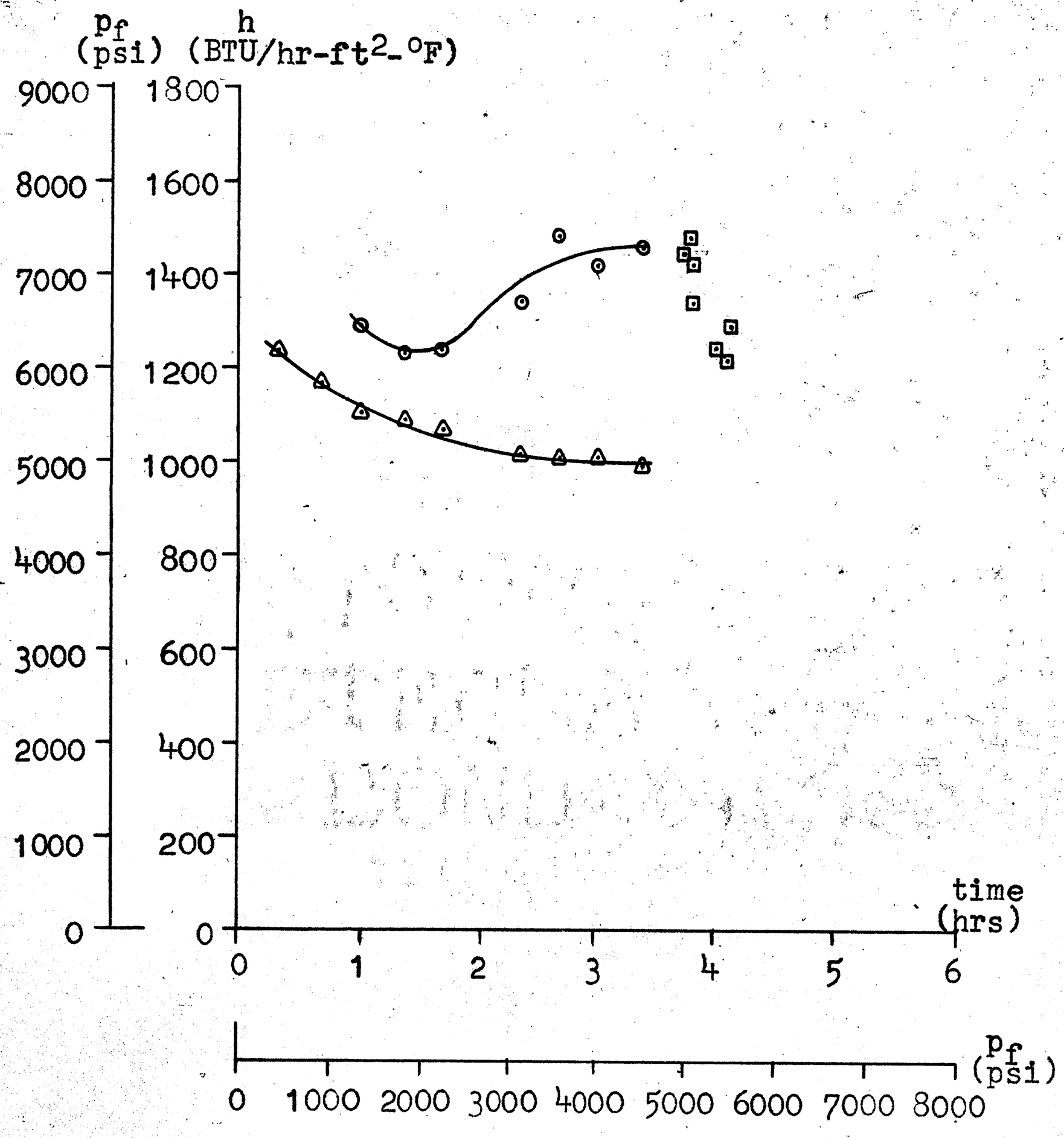

FIGURE 11

Transient Response of Conductance and Pressure and Conductance versus Pressure - Run Number 3

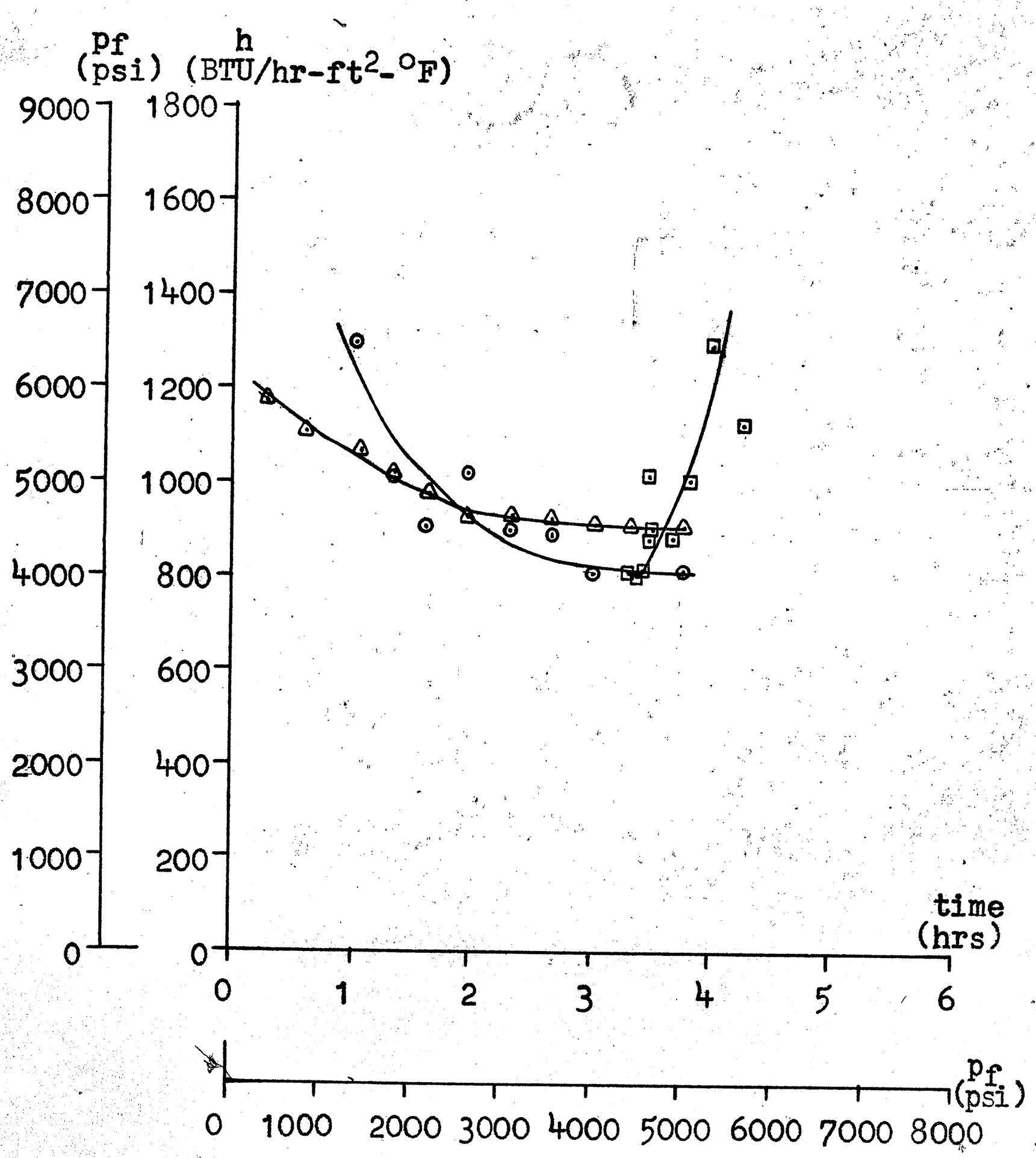

FIGURE 12

Transient Response of Conductance and Pressure and Conductance versus Pressure - Run Number 4

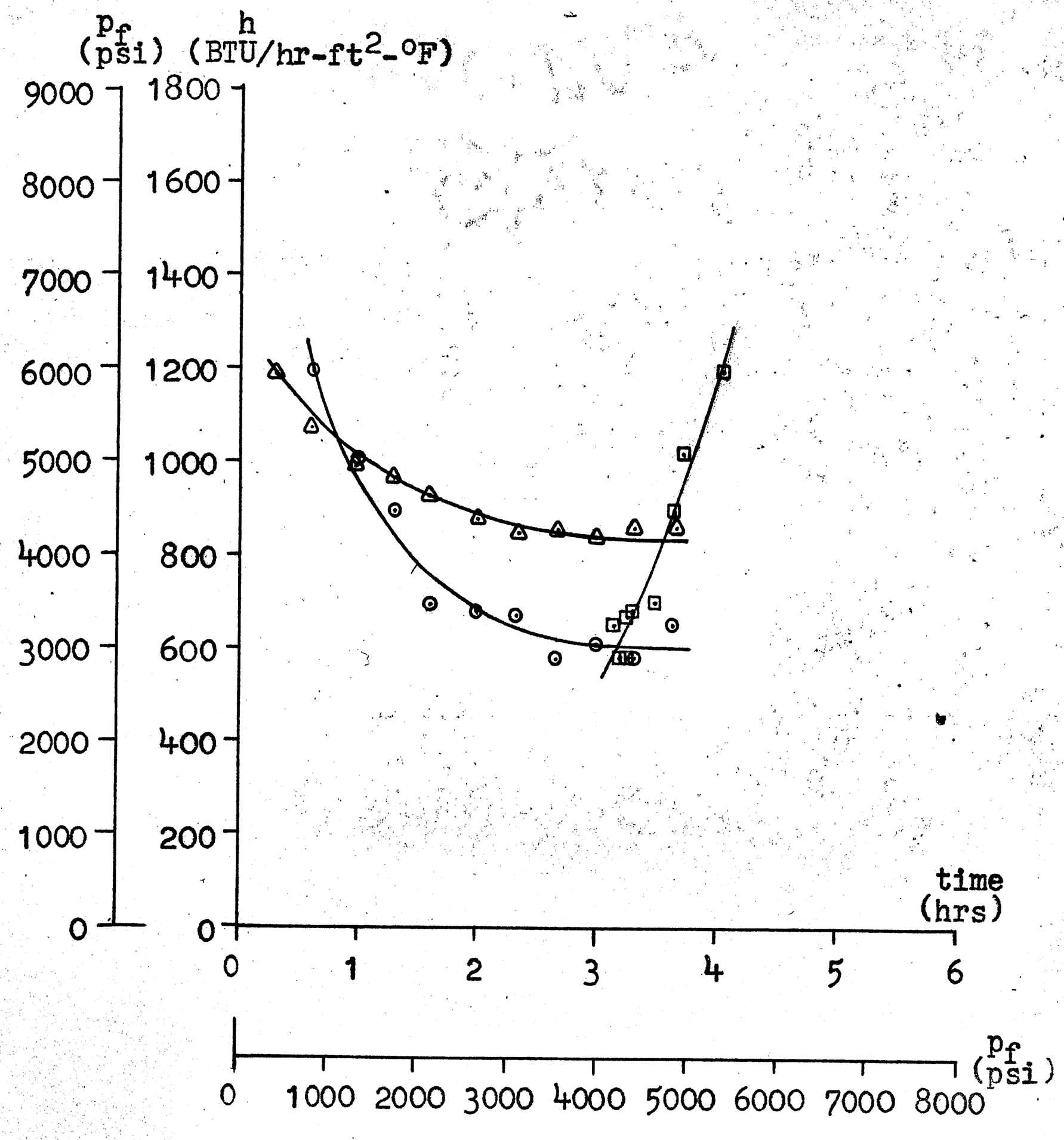

FIGURE 13

Transient Response of Conductance and Pressure and Conductance versus Pressure - Run Number 5

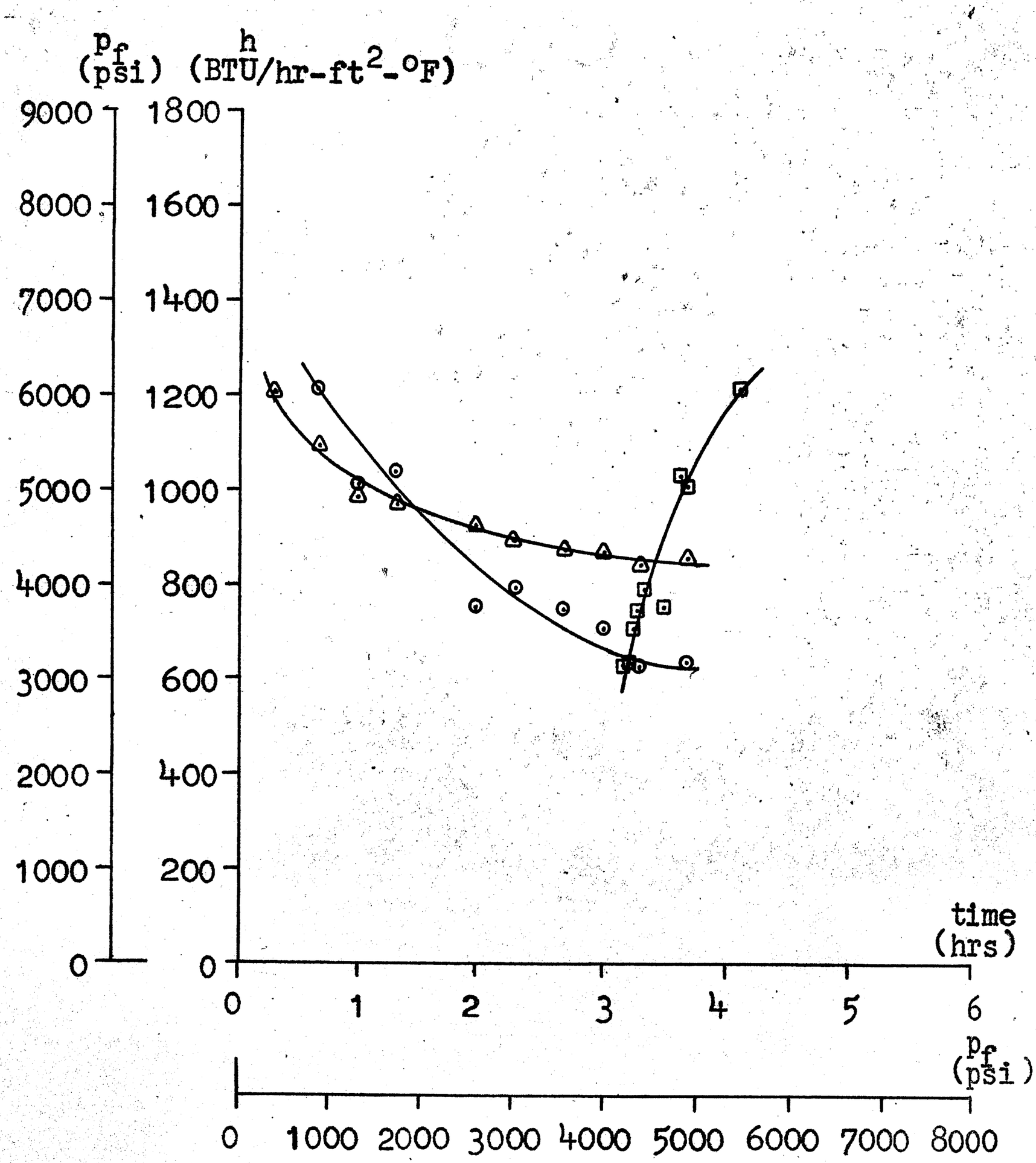

FIGURE 14

Transient Response of Conductance and Pressure and Conductance versus Pressure - Run Number 6

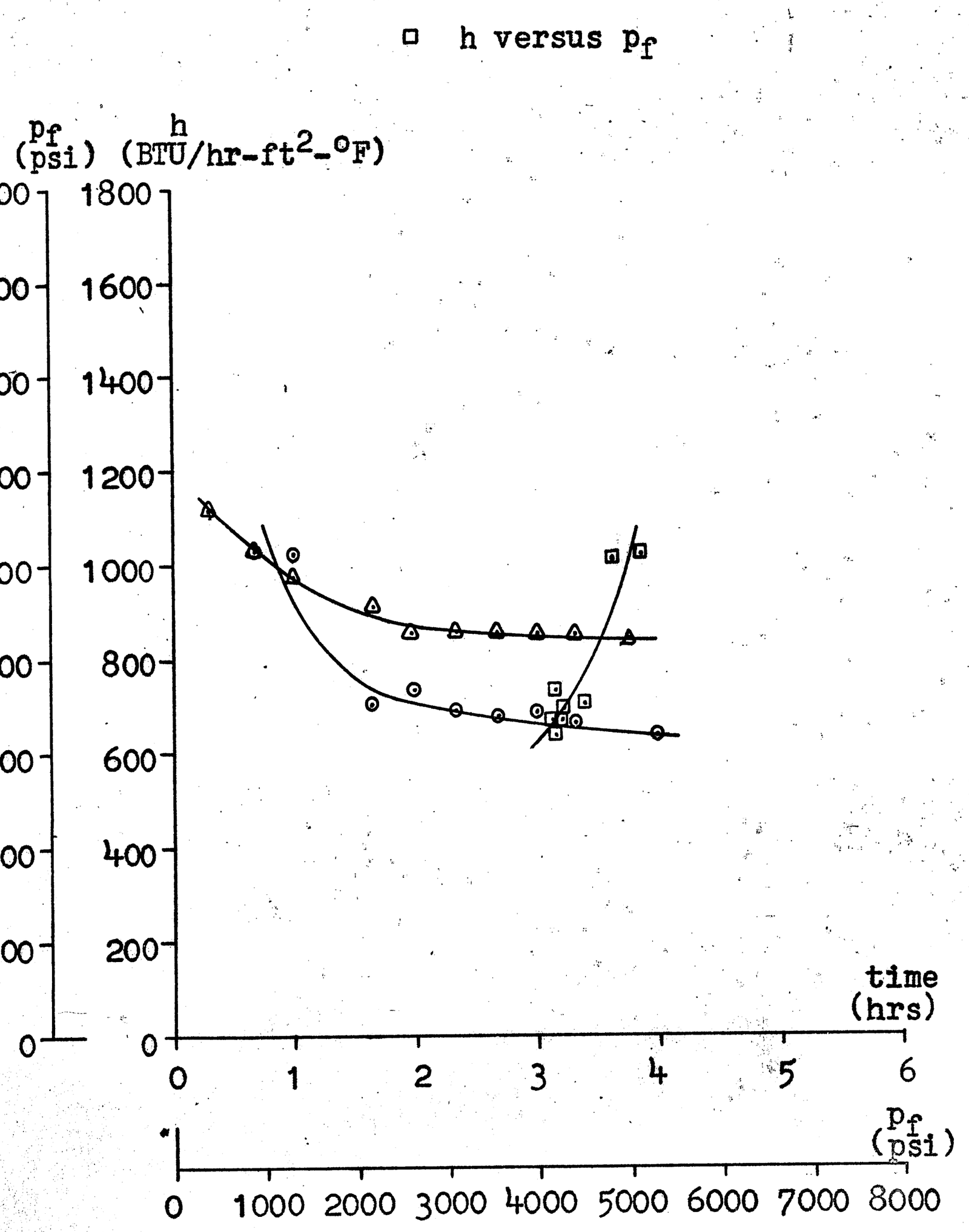

FIGURE 15

Transient Response of Conductance and Pressure and Conductance versus Pressure - Run Number 7

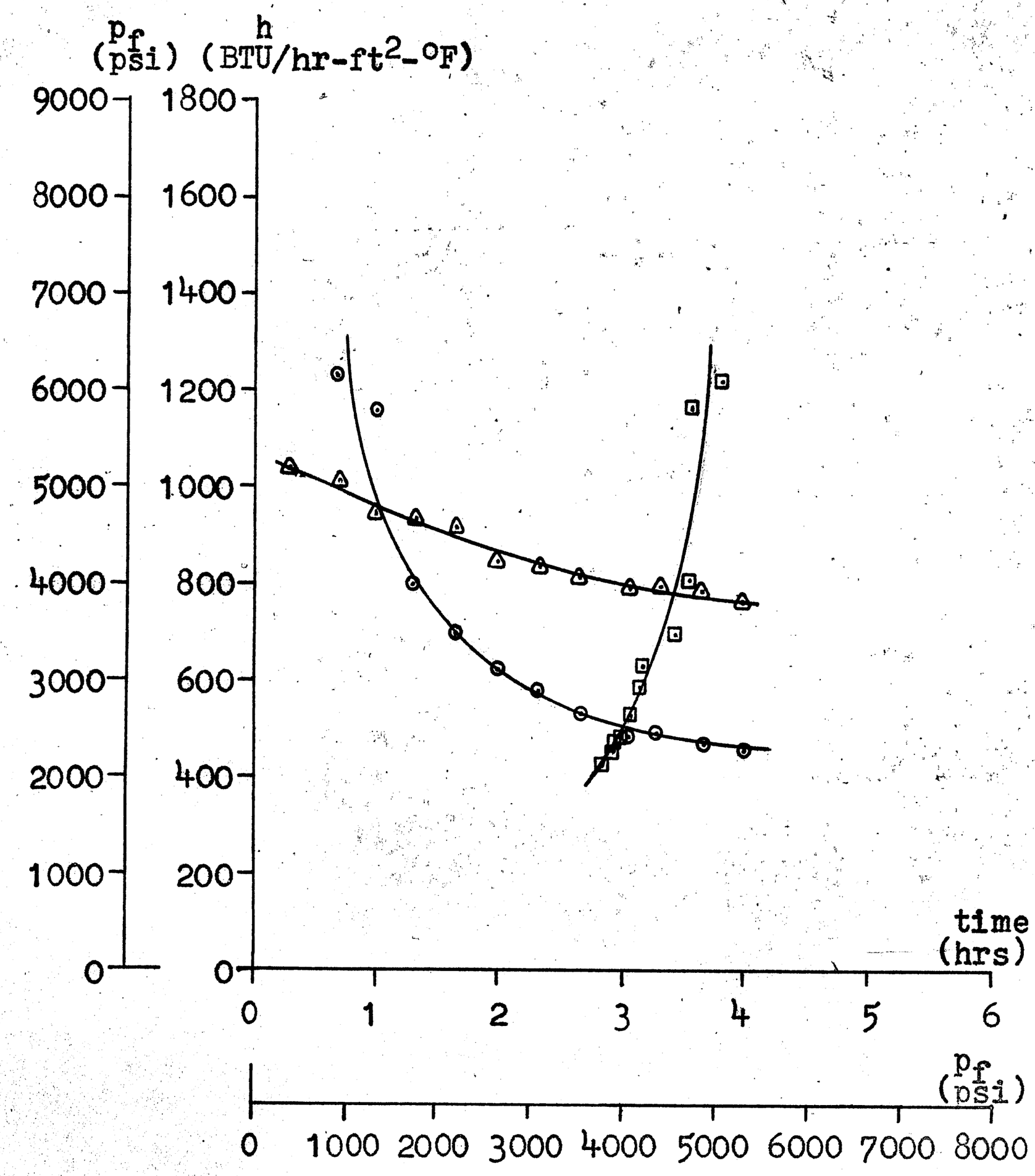

FIGURE 16

Transient Response of Conductance and Pressure and Conductance versus Pressure - Run Number 8

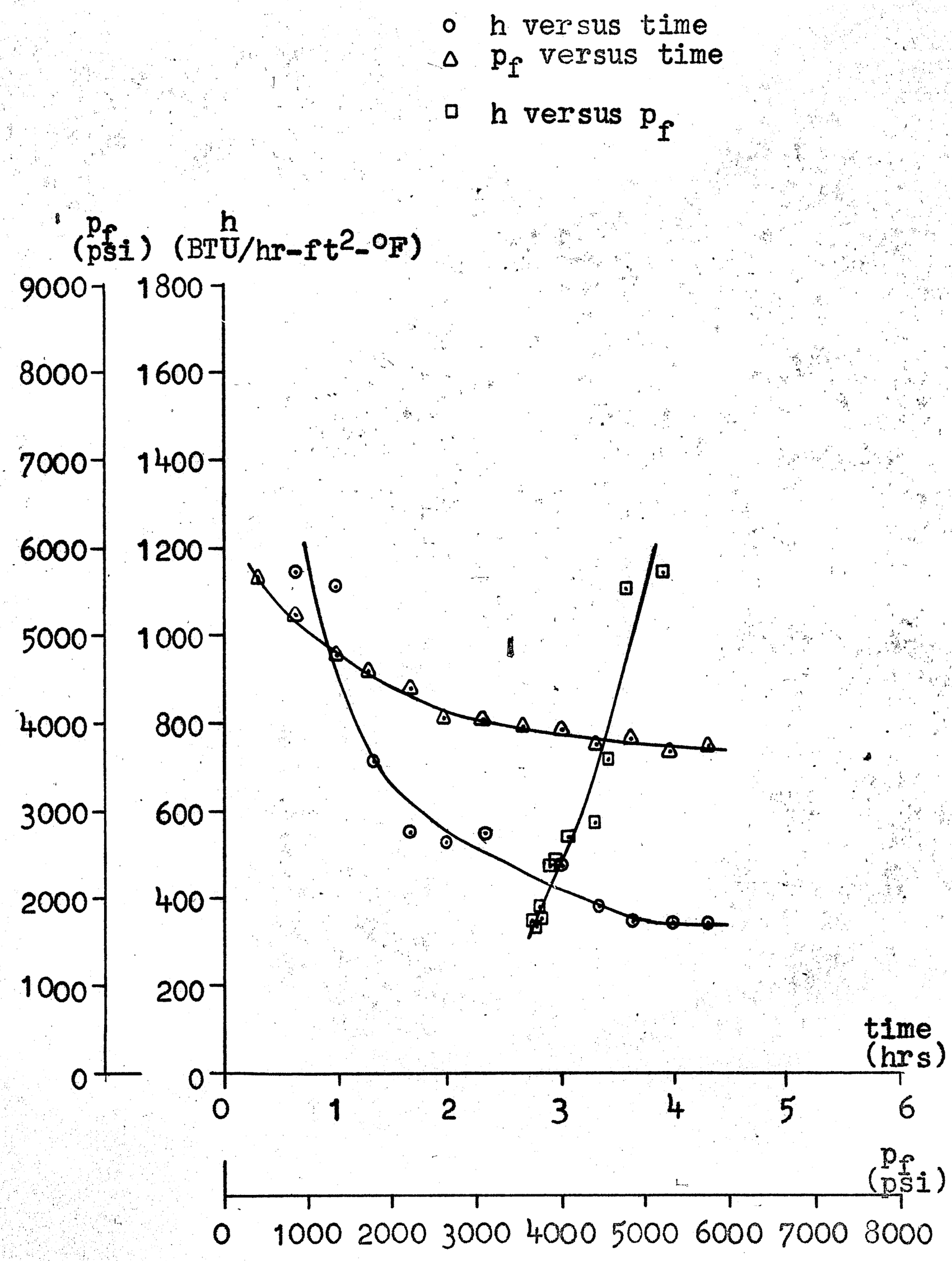

FIGURE 17

Transient Response of Conductance and Pressure and Conductance versus Pressure - Run Number 9

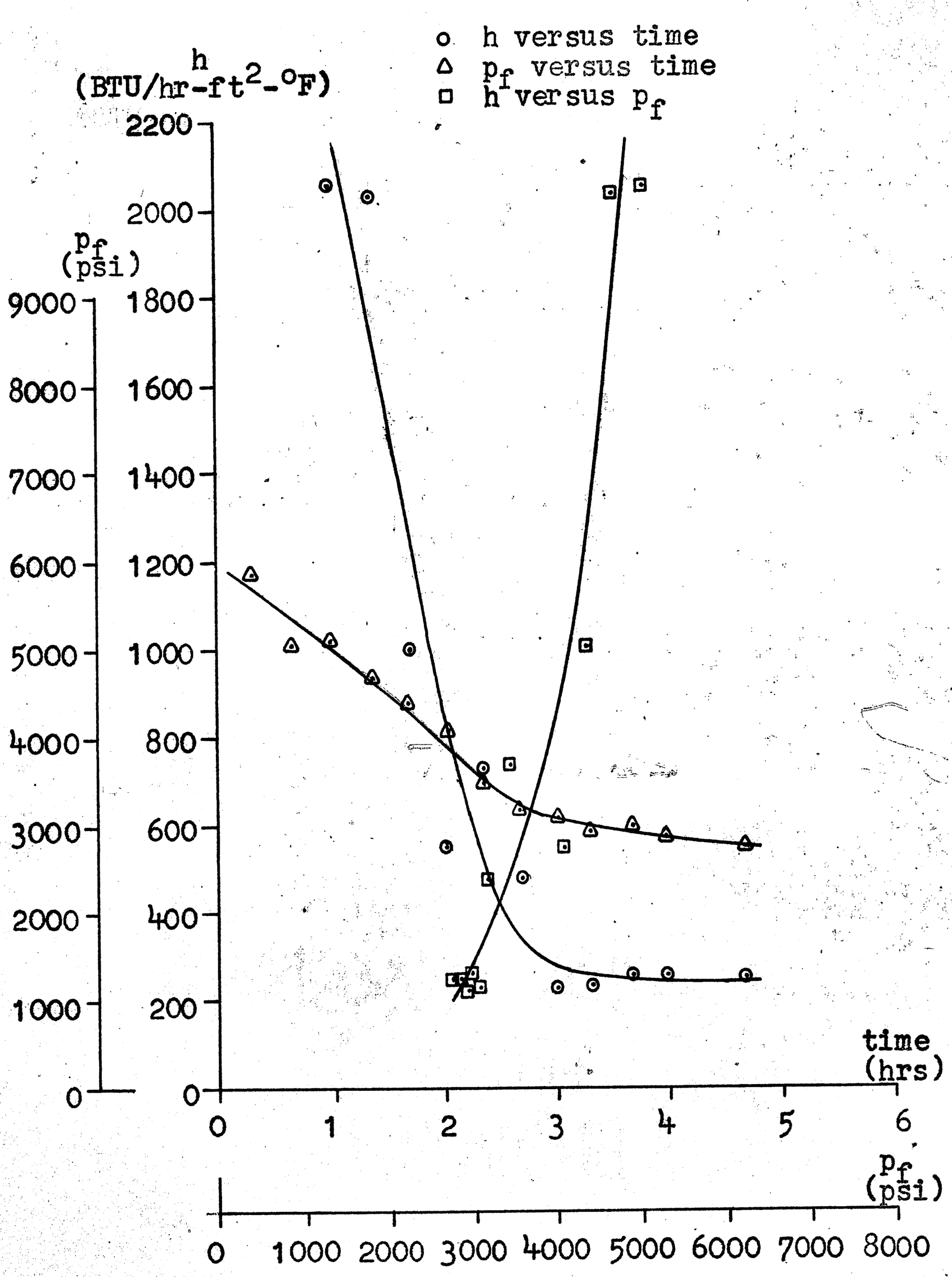

FIGURE 18

Transient Response of Conductance and Pressure and Conductance versus Pressure - Run Number 10

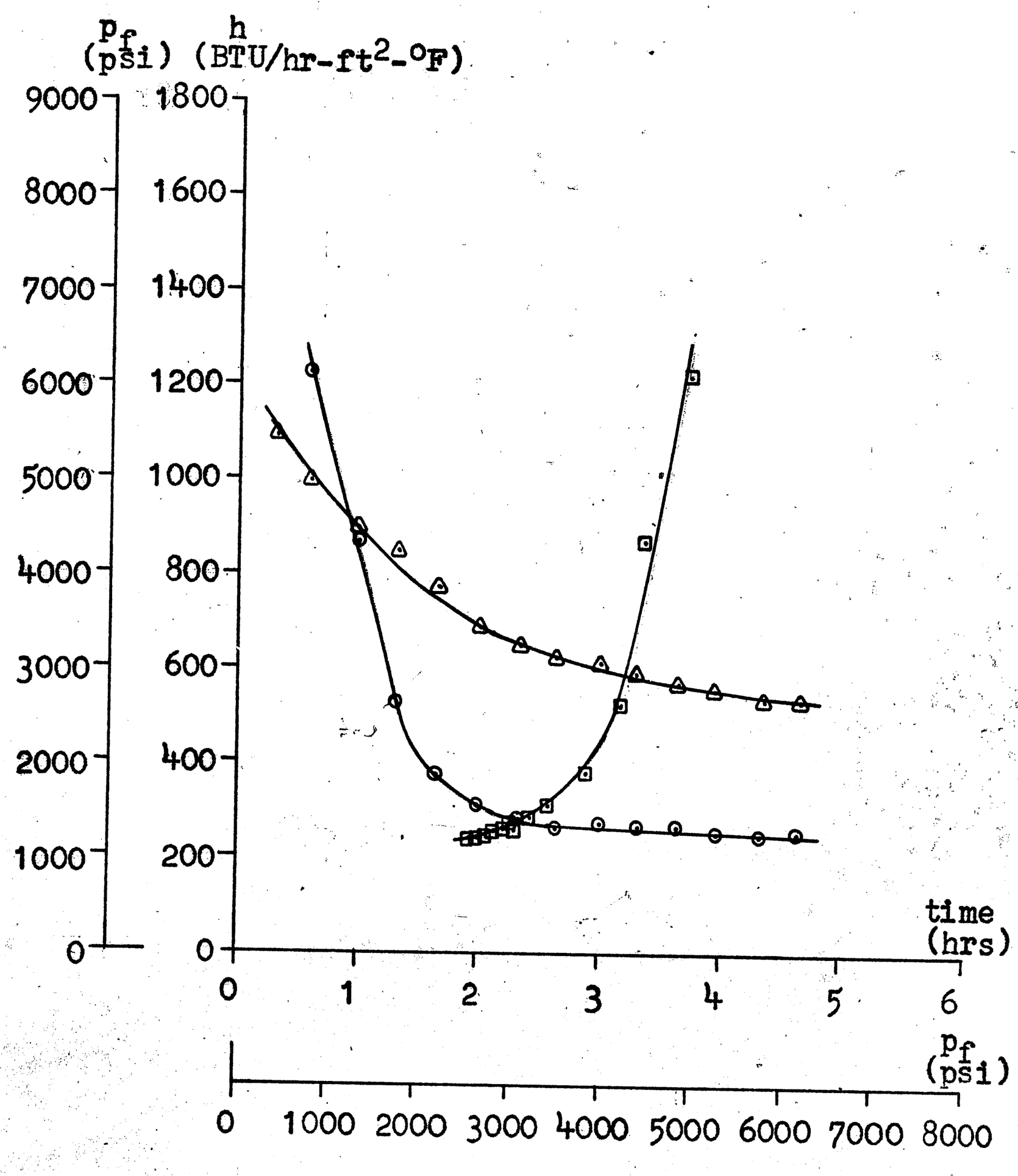

FIGURE 19

Transient Response of Conductance and Pressure and Conductance versus Pressure - Run Number 11

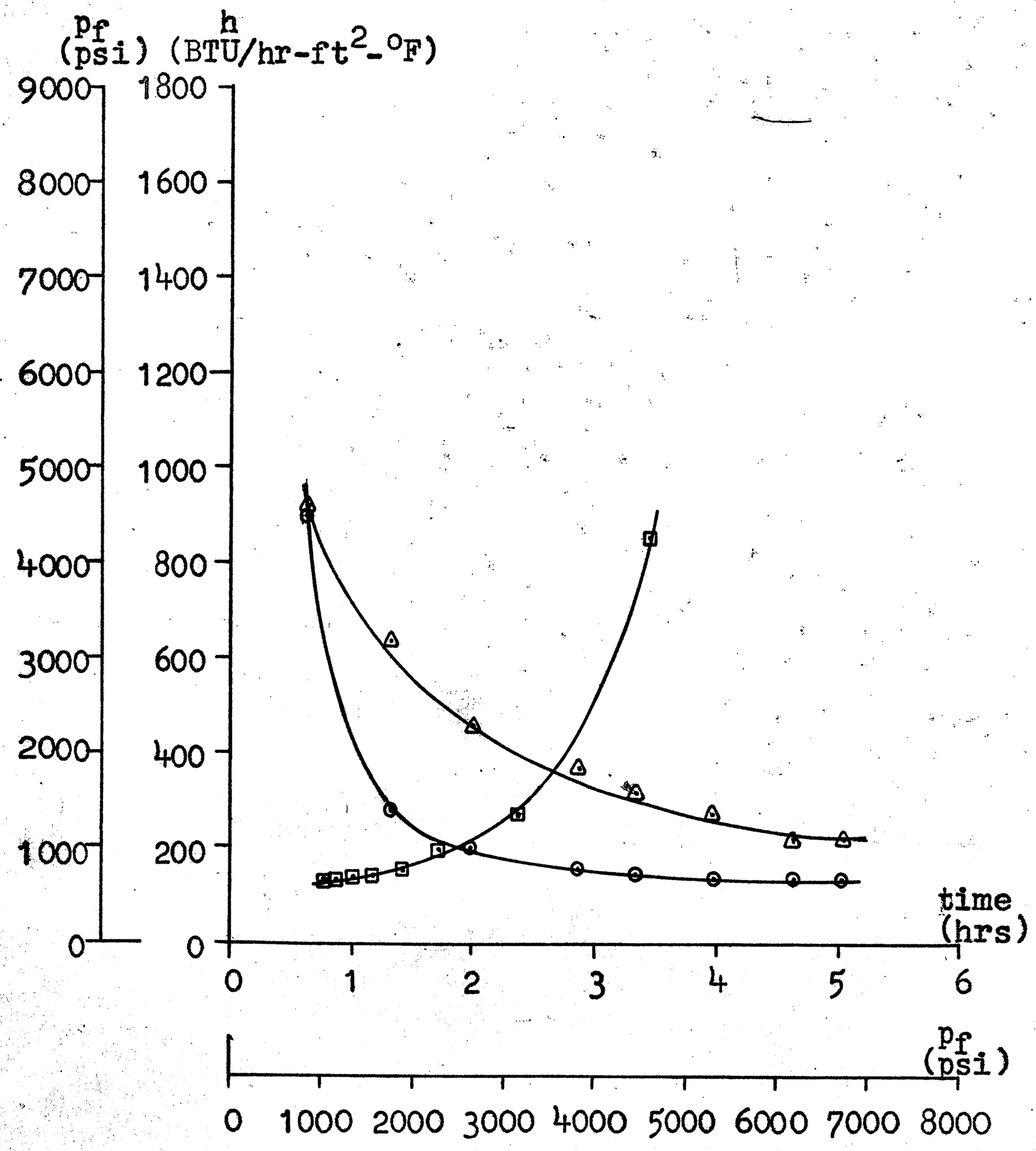

FIGURE 20

Transient Response of Conductance and Pressure and Conductance versus Pressure - Run Number 13

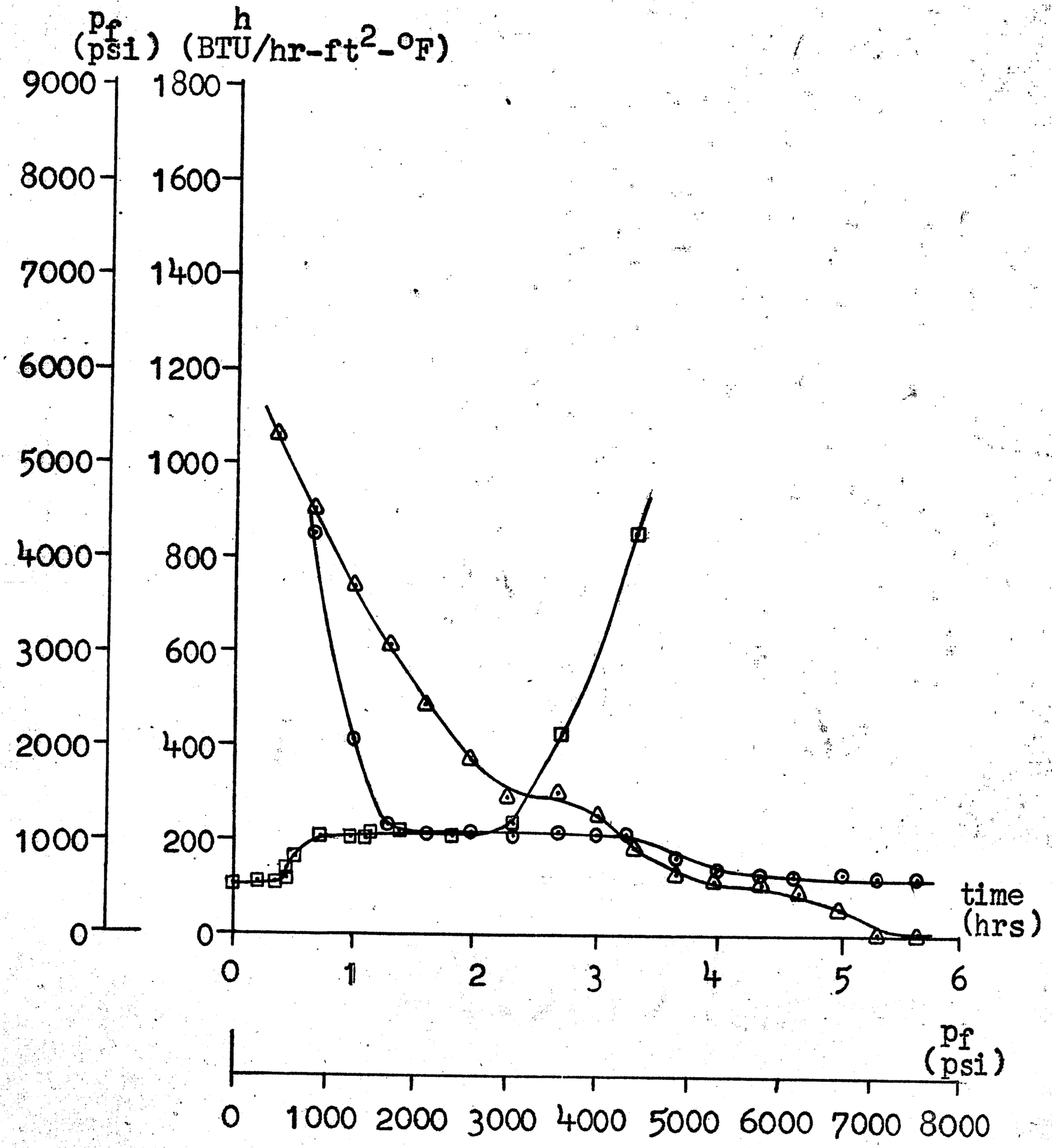

FIGURE 21

Conductance versus Pressure
Induced by Axial Loading - Runs Number 12 and 14

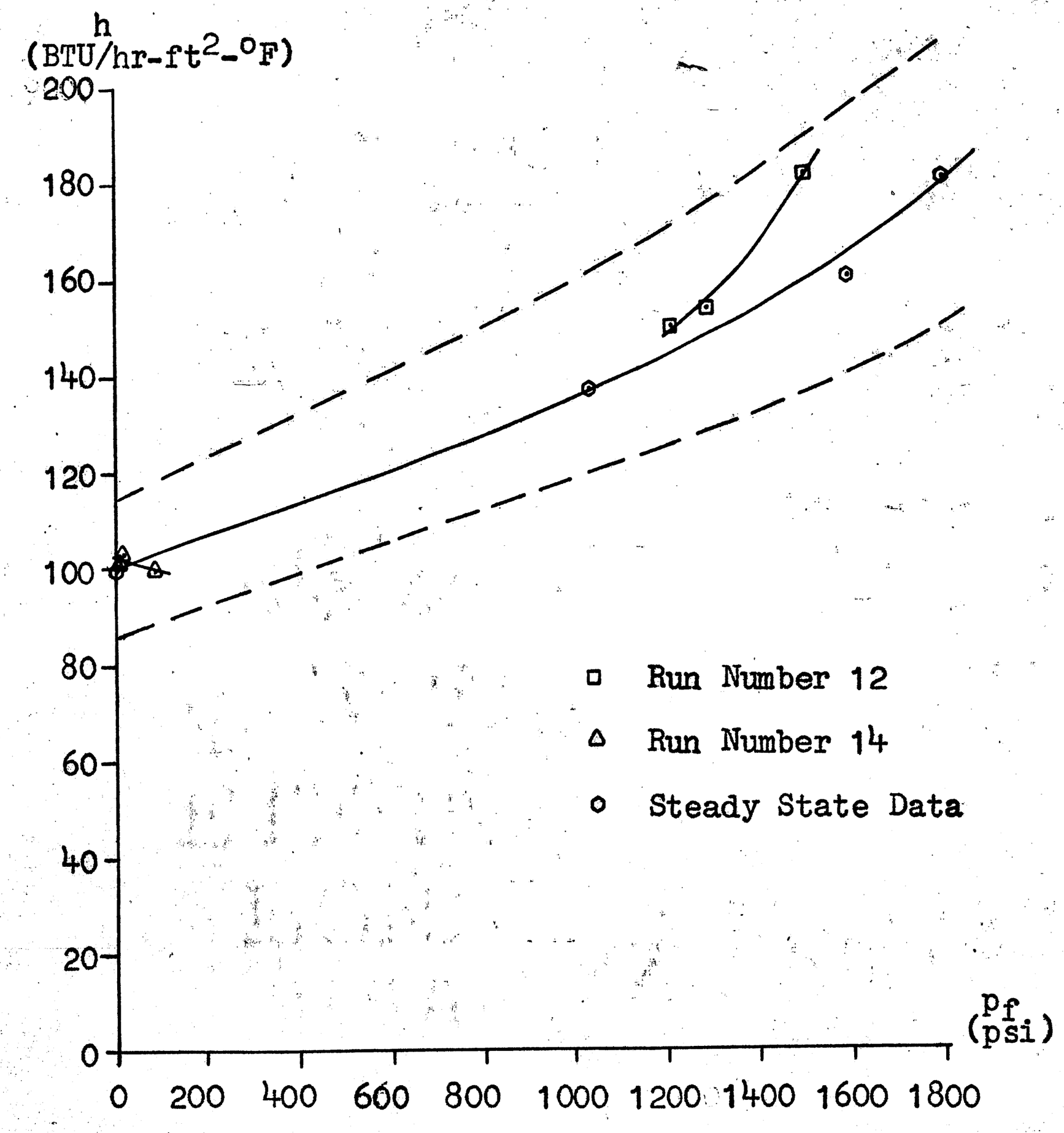

VIII. DISCUSSION OF EXPERIMENTAL DESIGN AND OPERATION

Some of the areas touched on previously need to be discussed more fully and, in some cases, modified. These are the areas of thermocouple location, diametrical interference, interface pressure, and curve fitting temperatures.

The thermocouple locations which were to be used originally placed the number 4 and 5 thermocouples .20 inch from the interface with a .50 inch spacing between thermocouples. However, due to flexing of the twist drills used in drilling the thermocouple holes, the holes obtained were not vertical. Accounting for this deviation from vertical resulted in the final thermocouple locations listed in Figure 2 except for thermocouples 4 and 5. Thermocouples 4 and 5 were relocated closer to each other and the joint because of initial difficulties experienced in determining joint conductances.

A critical part of the experiment was the determination of the diametrical interference, which fixed the initial interface pressure and greatly influenced all operating pressures. The theoretical procedure used to determine this interference has been discussed in Chapter 3. However, when the interface pressure was calculated from equation (2-12) utilizing steady state temperature

profiles from run number 13 (the run with the highest heat input), the theoretically determined interference of .0032 inches resulted in a negative interface pressure. Obviously, the interference was more than the supposed .0032 inches. This was quite possible since there was difficulty in holding the necessary dimensions in the machining process.

To get the actual interference, equation (2-12) was used with the steady state temperature profiles from run number 13 and an interface pressure of 6 psi. This equation was solved for the outside radius of the inner cylinder, which effectively gave an interference of .00491 inches and an initial interface pressure of 7830 psi. It should be noted that the 6 psi interface pressure was obtained from a consideration of the friction force between the two cylinders. That is, at the heat input of run number 13, the two cylinders had just started to slip apart. Knowing the coefficient of friction, the weight of the outside cylinder, and the interface area, it was possible to calculate the normal force and hence, the interface pressure of 6 psi.

A check on the interference was made by utilizing the hoop strain gage. A reading was taken at room temperature and then the outside cylinder was cut off. A final reading was taken and the difference in readings

computed. The result was 540 micro-inches/inch strain. This compared favorably and within the strain gage limits of error, it was felt, to the 553 micro-inches/inch strain which corresponded to the interference of .00491.

Two methods of calculating interface pressure were presented. One utilized temperature profiles on each side of the joint (equation (2-12)), and the other used the temperature profile in the inside cylinder plus a known hoop stress (equation (2-13)). The pressures which appear in the results have been calculated by the former method. This method was used because it was found to be insensitive to temperature changes at one particular location. That is, it depended upon two temperature profiles determined by eight individual measurements; and any error in one thermocouple reading would not greatly affect the temperature profile.

The second method, on the other hand, substituted a hoop stress for a temperature profile. Since this hoop stress was determined by a single strain gage, any error would directly affect the interface pressure. Furthermore, because of the nature of the small strains and corresponding stresses, it was felt the percentage error in recorded strains was on the order of 20 percent, whereas error in temperatures was less than 1 percent. Since interface pressure would reflect these

errors, the first method (equation (2-12)) was relied upon.

The calculation of joint conductance involved the curve fitting of temperature data. First, second, and third order fits were tried; and, as stated previously, a second order fit was finally used. The reason for selecting a second order fit was chiefly that the temperature gradients at the joint reflected the heat input. That is, the heat flowing thru the joint, as calculated from the temperature gradients, was less than the known heat input and compared favorably (within limits of error) with a heat balance on the cooling water. The temperature gradients of the first order fits were also similar to those of the second order. Surprisingly, the third order fits resulted in temperature gradients which predicted more heat crossing the joint then was being put in the test specimen by the heater. What was probably happening was that in order to fit the data points exactly, the curve outside the data points was greatly distorted, resulting in very high temperature gradients at the joint. Therefore, the second order fits were relied upon because they could be extrapolated to the the joint without much distortion.

IX. DISCUSSION OF RESULTS

The results of the experiment, namely joint conductances and pressures, are tabulated in Tables 1 thru 14 and have been used to establish the plots found in Figures 7 thru 21.

An important assumption used in arriving at the joint conductance versus pressure plots was that the joint conductance was independent of joint temperatures over the temperature range operated in. This assumption was necessary because of the principal method used to vary pressure. As previously described in Chapter 3, this method involved varying the heat input which changed the temperature profile which in turn created a differential expansion and changed the joint pressure. Obviously, because of the changing temperature profiles, the mean joint temperature was not constant. For the range of heat inputs considered, it was found to vary between 164 and 276 ^{o}F.

The assumption made above was not without basis. Two previous investigations, one by W. B. Kouwenhoven and J. H. Potter [2] and one by N. D. Weills and E. A. Ryder [4] had looked at joint conductance between two rough steel surfaces as a function of joint temperatures. Both investigations indicate that temperature has a very small effect on thermal conductance - on the order of

10 BTU/hr-ft^2-^{o}F per 100 ^{o}F. Since the variation of the mean joint temperature was only 112 ^{o}F, it was felt that the assumption of joint conduction being independent of temperature was justified.

With the above assumption in effect, the main objective of this investigation (the determination of pressure effects on joint conductance) could be achieved. The variation of joint conductance with pressure appears in Figure 7. The two dotted lines on either side of the conductance plot represent the limits of experimental error. These limits were arrived at by considering the errors present in the temperature gradient at the joint and the temperature drop across the joint. By comparing heat fluxes at various points, it was felt that the temperature gradient was accurate to within $\pm$8 percent. The error in temperature drop across the joint varied between 4.5 percent and 100 percent.[3] Because the low

---

3. A note of explanation is obviously necessary here. It has been stated previously that Conax certifies the accuracy of their thermocouples to $\pm$1.2 ^{o}F in the temperature range operated in. Since the temperature drop across the joint is essentially determined by the difference in temperatures between two thermocouples, numbers 4 and 5, the error in the temperature drop would be approximately $\pm$2.4 ^{o}F, neglecting all extrapolation error. Now if the temperature drop is 60 ^{o}F, the percentage error is 4.5 percent; and if it is less than 3 ^{o}F, the percentage error approaches 100 percent.

joint conductance values were characterized by high temperature drops across the joint, the error in the joint conductance is about 12.5 percent at low pressures and the limits of error in Figure 7 lie close to the conductance curve. Higher conductance values were characterized by smaller temperature drops and increasing error which results in the diverging limits of error shown in Figure 7.

In Figure 7 are shown the steady state results of joint conductance versus interface pressure. The behavior is as expected - conductance increasing with increasing pressure. Furthermore, all the data points plotted lie within the limits of experimental error.

The plot which appears in Figure 8 contains all the data points recorded. Again the dotted lines represent the limits of experimental error. Interestingly enough, practically all the plotted points fall within this band. It is felt that this plot provides an indication of the overall accuracy of the results as well as a vindication of the experimental techniques employed and the assumptions made. It is also felt that the experimental scatter found in the region of high joint pressures indicates that the experimental error in this region is less than that predicted.

Figures 9 thru 20 contain the transient responses

of interface pressure and joint conductance for a fixed heat input along with joint conductance plotted as a function of interface pressure. The trends exhibited in these plots are essentially similar, the exceptions being Figures 1 and 2. The joint conductance data appearing in these figures were obtained from low heat inputs. Hence, the temperature drops across the joint were also low and the data scatter very great. For this reason no attempt was made to fit a curve to the conductance versus pressure data in Figures 1 and 2. From Figure 3 on there is considerably less scatter and curves can be fitted.

In all the figures the initial conductance value obtained after the first 20 minutes of operation, and in some cases after 40 minutes of operation, is not plotted. This was because the temperatures in the cylinders during start up were changing too rapidly, and an accurate temperature profile could not be established. This is also reflected by the increasing values of joint conductance (in tables) instead of the expected decreasing trend. From 40 minutes on, the expected profile was obtained.

An interesting observation which can be made in these figures is the smoothness of the transient pressure responses with very little scatter. It is felt

that this is an indication of the accuracy of the technique used to calculate interface pressures.

The remaining figure, Figure 21, is a plot of joint conductance versus interface pressure. The data used in plotting this curve was obtained by the second method described in Chapter 3. That is, the inner cylinder was compressed to increase the interface pressure with the heat input and mean interface temperature remaining constant. Two sets of data have been plotted. Only one set of data establishes a trend, the other set of data being taken while the two cylinders had begun to slip apart and, therefore, is questionable. However, the trend established by the single plot corresponds closely to the conductance plot of Figure 7, which is shown in Figure 21 for comparison purposes. All the points lie within the experimental limits of error. The apparent compatability between the two methods of changing interface pressure and joint conductance lends further credance to the results.

X. CONCLUSIONS AND RECOMMENDATIONS

FURTHER STUDY

The trends obtained were exactly as expected. The joint conductance and interface pressure decreased with time for a fixed heat input. In all cases, joint conductance increased with an increase in the interface pressure. These trends are similar to those recorded by other experimenters using plane surface geometry.

Because of the dependence of conductance on a variety of variables, no serious attempt was made to correlate the results to those of other investigators. The closest one-dimensional investigation was that of A. W. Brunot and Florence F. Buckland [3], who investigated a milled steel joint with a surface roughness of 125 micro-inches. Their values for joint conductance ranged from 247 BTU/hr-ft^2-^{o}F at approximately 5 psi to 550 BTU/hr-ft^2-^{o}F at 300 psi. The values of joint conductance which were obtained in this investigation at similar pressures are 109 and 120 BTU/hr-ft^2-^{o}F. These values are considerably different, but then so are many of the test variables.

Any future work done with the geometry used in this experiment should retain the Poisson effect to vary the interface pressure. Although little data was obtained by this technique, a larger compressive test-

ing machine would increase its useful range, and interface temperature effects could be completely eliminated by fixing the heat input and using the testing machine to vary interface pressure.

One area which could be improved is the technique of calculating initial interface pressure. The interface pressure is extremely sensitive to diametrical interference and must be precisely determined to establish a base for calculating operating pressures. Also, different materials should be substituted for the steel cylinders used in this investigation.

XI. APPENDICES

A. Variable Notation and Values

quantity	description	value (if fixed)
$\dot{q}$	heat flow per unit time	
k	thermal conductivity	26 BTU/hr-ft-^{o}F
A_j	interface area	81.7 in^2
$(dT/dr)_j$	temperature gradient at the joint	
h	joint conductance	
$(\Delta T)_j$	temperature drop across the joint	
b_o	inside radius of the outer cylinder	3.25 in
p_o	pressure on the outside surface of the outer cylinder	14.7 psi
E_o	modulus of elasticity of the outer cylinder	30 x 10^6
c	outside radius of the outer cylinder	6.25 in
b_i	outside radius of the inner cylinder	3.252455 in
p_i	pressure on the inner surface of the inner cylinder	16 psi
E_i	modulus of elasticity of the inner cylinder	30 x 10^6
a	inside radius of the inner cylinder	.875 in
p_f	interface pressure	
ϑ_o	Poisson's ratio for the outside cylinder	.26

quantity	description	value (if fixed)
ν_i	Poisson's ratio for the inside cylinder	.26
T	temperature distribtion	
α_o	coefficient of thermal expansion for the outside cylinder	6.4×10^{-6} in/in-^oF
α_i	coefficient of thermal expansion for the inside cylinder	6.4×10^{-6} in/in-^oF
L	compressive load applied to the inside cylinder	
σ_H	hoop stress	

B. Test Equipment

1. Eight copper-constantan Conax thermocouples, no. T-SS4-G-T3-MIC-040-AT-3

2. Leeds and Northrup, no. 8686 Millivolt Potentiometer and switching unit

3. two Micro-Measurements strain gages, EA-06-250AF-120

4. Baldwin-Lima-Hamilton SR-4 indicator, model 120-C

5. Two Fischer mercury thermometers, readable to 1/4 ^{o}F

6. One Baldwin 60,000 pound testing machine

C. Condensed Data

RUN NUMBER 1

heat input: 1970 BTU/hr

cooling water flow rate: 626 lb_m/hr

cooling water temperature
in: 61.5 °F
out: 64.5 °F

thermocouplesreadings in °F:

time	thermocouple number							
	1	2	3	4	5	6	7	8
0	87.78	———						→
:20	96.33	99.52	103.22	108.39	110.00	112.10	114.29	119.62
:40	113.12	117.62	122.50	129.54	131.33	134.38	137.71	143.64
1:00	122.37	128.08	133.76	141.88	143.96	148.21	151.80	158.12
1:20	128.67	134.79	140.88	149.33	151.50	156.40	160.42	167.08
1:40	133.37	139.62	145.52	154.08	156.28	161.32	165.48	172.52
2:00	134.75	141.40	148.04	157.42	159.56	164.92	169.36	176.36
2:20	138.72	144.54	151.21	160.25	163.00	167.96	172.60	179.36
2:40	138.92	145.24	152.00	161.16	163.88	168.88	173.36	180.48
3:00	138.88	146.00	153.00	162.68	165.08	170.44	174.84	181.88
3:20	141.08	147.48	154.16	163.60	166.08	171.52	176.04	183.20

RUN NUMBER 2

heat input: 2550 BTU/hr

cooling water flow rate: 636 lb_m/hr

cooling water temperature
in: 62 °F
out: 66 °F

Thermocouple readings in °F:

time	thermocouple number							
	1	2	3	4	5	6	7	8
0	75.83	———						→
:20	95.39	99.00	103.39	109.87	112.13	115.33	118.87	126.30
:40	118.87	123.75	129.37	137.80	140.79	145.84	149.54	157.75
1:00	132.83	138.28	144.96	155.21	158.44	165.24	169.68	178.00
1:20	141.52	148.12	155.21	166.36	169.76	177.60	182.50	191.04
1:40	147.88	155.04	162.24	173.88	177.32	185.65	190.80	199.92
2:00	149.41	157.37	165.40	178.77	181.76	190.80	196.23	205.15
2:20	153.96	161.96	169.96	182.84	186.80	196.11	201.48	210.85
2:40	155.92	164.36	172.56	185.81	189.58	199.12	204.46	213.69
3:00	157.96	166.04	174.12	187.08	191.04	200.73	206.15	215.38
3:20	156.56	165.52	174.08	187.58	191.52	201.40	206.88	216.15

RUN NUMBER 3

heat input: 2870 BTU/hr

cooling water flow rate: 628 lb_m/hr

cooling water temperature
in: 61.5 °F
out: 65 °F

thermocouple readings in °F:

	thermocouple number							
time	1	2	3	4	5	6	7	8
0	73.55	→						
:20	101.17	104.87	109.50	116.61	119.48	123.71	127.12	135.87
:40	126.61	132.46	138.68	148.50	151.42	157.17	161.16	168.92
1:00	141.56	148.96	156.46	168.00	171.36	178.61	183.44	192.08
1:20	151.46	159.32	167.12	179.85	184.16	192.72	198.35	208.04
1:40	158.76	167.08	175.20	188.44	193.38	202.65	208.80	219.15
2:00	159.92	169.16	178.27	192.60	198.38	207.69	213.89	224.19
2:20	163.96	172.64	181.24	195.04	200.85	210.73	216.89	227.27
2:40	165.40	174.72	183.76	198.00	204.00	213.92	220.15	230.50
3:00	167.52	176.72	185.69	199.96	206.54	216.67	222.89	233.48
3:20	167.32	176.80	186.00	200.69	207.46	217.85	224.30	234.85
3:40	168.60	178.15	187.42	201.68	208.04	217.92	224.56	235.04

RUN NUMBER 4

heat input: 2930 BTU/hr

cooling water flow rate: 616 lb_m/hr

cooling water temperature
in: 64.5 °F
out: 68 °F

thermocouple readings in °F:

	thermocouple number							
time	1	2	3	4	5	6	7	8
0	83.0	—	—	—	—	—	—	→
:20	106.91	110.83	115.54	122.88	125.25	128.83	132.42	140.83
:40	134.75	140.83	147.44	157.96	161.12	167.16	173.08	181.64
1:00	151.62	158.92	166.60	179.04	183.24	191.48	197.00	207.38
1:20	161.16	169.36	177.72	191.32	196.69	205.92	211.81	222.57
1:40	165.32	174.32	183.48	197.76	204.54	214.58	222.81	231.58
2:00	169.00	178.92	188.48	203.15	210.62	220.65	227.00	238.00
2:20	170.32	180.72	190.56	205.77	213.69	224.15	230.42	241.37
2:40	172.96	184.96	193.00	207.92	216.04	226.48	232.74	243.69
3:00	173.48	183.92	193.69	208.84	217.27	227.77	234.12	245.74
3:20	174.52	184.84	194.65	209.38	218.23	228.85	235.11	246.11
3:40	175.72	185.62	195.44	210.77	219.19	229.89	236.22	247.26

RUN NUMBER 5

heat input: 3100 BTU/hr

cooling water flow rate: 628 lb_m/hr

cooling water temperature
in: 62 °F
out: 65.5 °F

thermocouple readings in °F:

time	thermocouple number							
	1	2	3	4	5	6	7	8
0	83.18	———						→
:20	107.04	111.63	116.56	124.46	126.70	138.96	134.52	141.80
:40	130.25	137.25	144.29	155.21	158.20	164.60	168.92	177.40
1:00	147.96	156.40	164.00	176.36	180.48	189.04	194.85	205.54
1:20	158.48	167.44	176.24	190.40	194.81	203.81	209.81	220.73
1:40	———	———	———	———	———	———	———	———
2:00	168.92	178.54	187.96	202.65	208.80	218.42	224.63	235.52
2:20	170.76	180.84	190.56	205.65	212.31	222.46	228.62	239.48
2:40	170.36	180.60	190.56	205.92	213.46	224.74	230.42	241.48
3:00	173.32	183.12	192.64	207.62	215.39	226.14	232.58	243.54
3:20	171.40	182.77	192.20	207.69	215.96	226.74	233.41	244.63
3:40	173.48	183.88	193.89	208.84	216.89	227.19	233.70	244.78

RUN NUMBER 6

heat input: 3150 BTU/hr

cooling water flow rate: 624 lb_m/hr

cooling water temperature
in: 61.5 °F
out: 66.5 °F

thermocouple readings in °F:

time	thermocouple number							
	1	2	3	4	5	6	7	8
0	85.26	→						
:20	104.74	109.54	114.62	122.29	124.71	128.83	133.08	143.92
:40	132.50	139.50	146.62	158.12	161.56	169.00	174.24	184.52
1:00	149.15	157.42	165.96	179.04	183.28	191.72	197.60	208.08
1:20	158.48	167.36	176.36	192.32	195.24	204.62	210.58	220.81
1:40	164.12	174.00	183.64	198.58	205.35	215.38	221.89	232.92
2:00	169.84	179.92	189.92	205.35	212.88	223.23	230.23	241.56
2:20	173.08	182.65	192.04	207.00	214.96	225.69	232.46	243.46
2:40	172.12	182.73	192.64	208.08	216.15	226.81	233.30	244.18
3:00	173.12	183.24	193.12	208.48	216.52	227.15	233.70	244.78
3:20	172.92	183.08	193.04	208.48	216.85	227.85	234.46	245.67
3:40	———	———	———	———	———	———	———	———
4:00	173.08	183.40	193.31	208.64	217.38	228.28	235.00	246.04

RUN NUMBER 7

heat input: 3270 BTU/hr

cooling water flow rate: 617 lb_m/hr

cooling water temperature
in: 62.5 °F
out: 68 °F

thermocouple readings in °F:

time	thermocouple number							
	1	2	3	4	5	6	7	8
0	98.17	———						→
:21	118.88	123.58	129.71	138.88	141.64	146.62	151.12	164.52
:40	139.88	146.88	154.36	166.60	170.08	177.88	183.08	193.58
1:00	155.83	163.52	172.20	186.00	190.52	199.65	205.73	216.71
1:20	164.72	173.60	182.46	196.62	202.42	212.27	218.54	229.74
1:40	173.28	182.46	191.32	205.77	212.35	222.23	228.62	239.89
2:00	175.04	184.68	194.27	209.50	218.08	228.61	235.22	246.65
2:20	178.20	188.20	197.76	212.73	221.62	232.15	238.85	250.41
2:40	179.64	189.58	199.35	214.62	224.67	235.52	242.22	253.89
3:02	178.85	189.54	199.58	215.35	226.44	237.42	244.22	255.85
3:22	180.08	190.32	200.35	215.81	226.81	237.88	244.67	256.30
3:40	180.68	191.12	201.16	216.70	228.31	239.56	246.42	258.22
4:00	178.73	189.54	199.92	216.00	228.65	239.89	246.73	258.44

RUN NUMBER 8

heat input: 3370 BTU/hr

cooling water flow rate: 625 lb_m/hr

cooling water temperature
in: 61.5 °F
out: 66 °F

thermocouple readings in °F:

time	thermocouple number							
	1	2	3	4	5	6	7	8
0	80	→						→
:20	105.54	109.75	114.67	123.04	125.71	129.96	134.12	144.42
:40	137.52	143.68	190.72	162.00	165.20	172.00	176.92	187.19
1:00	155.46	163.72	172.20	185.92	190.52	199.27	205.77	216.07
1:20	165.48	174.52	183.64	198.31	204.77	214.54	220.85	232.35
1:40	173.40	183.04	192.64	207.58	215.58	225.69	232.31	243.96
2:00	175.72	186.00	195.88	211.39	221.19	232.00	238.93	250.93
2:20	179.20	189.81	200.38	215.77	225.54	236.63	243.27	255.11
2:40	181.48	193.20	202.35	218.31	228.92	239.85	246.62	258.44
3:00	183.72	194.58	204.96	220.89	232.35	243.28	250.37	261.85
3:20	183.24	194.23	204.61	220.73	234.54	245.56	252.29	264.26
3:40	186.00	198.96	207.46	223.31	236.89	247.89	254.33	266.22
4:00	185.54	196.50	207.08	223.08	238.22	249.35	255.70	267.60
4:20	186.80	198.00	208.44	224.11	238.70	249.54	255.81	267.60

RUN NUMBER 9

heat input: 3560 BTU/hr

cooling water flow rate: 635 lb_m/hr

cooling water temperature:
in: 61 ^oF
out: 66.5 ^oF

thermocouple readings in ^oF:

	thermocouple number							
time	1	2	3	4	5	6	7	8
0	82.09	———						→
:20	108.22	112.78	118.43	126.57	128.75	132.83	136.63	145.27
:40	141.08	148.29	156.12	168.12	170.64	177.76	183.52	194.89
1:00	158.08	167.08	176.52	190.32	193.31	207.77	208.40	220.35
1:20	168.12	178.50	188.60	203.77	206.38	215.38	222.31	234.77
1:40	176.12	186.80	197.20	213.12	218.00	228.00	235.19	248.11
2:00	183.16	194.08	204.12	218.65	226.48	236.00	243.31	256.15
2:20	179.94	190.24	200.08	215.73	233.63	245.85	252.26	264.37
2:40	178.28	189.23	199.62	216.56	238.74	250.19	256.30	268.04
3:00	180.16	190.76	200.96	217.85	242.11	253.18	259.22	271.26
3:20	182.62	193.50	204.12	221.31	245.89	257.41	263.78	276.18
3:40	186.00	197.36	208.04	224.56	246.81	259.44	266.52	279.37
4:00	185.67	197.00	207.89	224.74	248.11	261.41	268.68	281.67
4:20	———	———	———	———	———	———	———	———
4:40	186.20	198.00	208.96	226.74	251.11	264.81	272.00	284.89

RUN NUMBER 10

heat input: 3650 BTU/hr

cooling water flow rate: 635 lb_m/hr

cooling water temperature
in: 63 °F
out: 68.5 °F

thermocouple readings in °F:

time	thermocouple number							
	1	2	3	4	5	6	7	8
0	84.17	———						→
:20	108.25	114.25	120.54	129.54	132.83	136.42	141.40	151.79
:40	142.12	149.17	157.04	169.60	173.12	180.92	186.28	197.28
1:00	159.28	168.20	177.56	192.24	198.04	207.31	213.65	225.11
1:20	171.00	180.76	190.72	206.42	215.42	225.69	232.35	244.52
1:40	176.32	187.00	197.48	213.77	226.18	237.00	243.88	256.48
2:00	179.52	190.60	201.28	217.69	234.50	245.59	252.22	264.85
2:20	182.69	193.50	204.65	220.96	240.81	252.44	259.74	271.55
2:40	184.33	195.92	206.69	223.35	244.48	256.67	263.48	275.89
3:00	186.00	197.60	208.56	225.15	246.54	259.48	266.59	278.89
3:20	186.60	198.23	209.31	226.44	248.74	261.85	268.75	281.37
3:40	187.23	198.96	210.19	227.61	251.12	264.67	271.78	284.21
4:00	188.40	200.12	211.35	228.58	252.74	266.44	273.52	286.21
4:20	189.54	200.69	211.46	228.27	253.78	267.89	275.11	287.96
4:40	187.61	199.92	211.48	229.26	254.70	268.75	276.00	288.75
*	190.12	201.80	213.27	230.96	259.44	273.67	280.36	292.39

*Note: This set of data was recorded at steady state for a heat input of 3820 BTU/hr and a cooling water exit temperature of 69 °F.

RUN NUMBER 11

heat input: 4000 BTU/hr

cooling water flow rate: 610 lb_m/hr

cooling water temperature
in: 63.5 °F
out: 70 °F

thermocouple readings in °F:

	thermocouple number							
time	1	2	3	4	5	6	7	8
0	81.65	———						→
:20	———	———	———	———	———	———	———	———
:40	145.84	154.36	163.00	176.84	181.88	190.80	196.54	209.04
1:00	———	———	———	———	———	———	———	———
1:20	175.68	185.77	195.88	212.12	231.38	243.38	250.19	264.07
1:40	———	———	———	———	———	———	———	———
2:00	185.46	197.00	207.92	225.31	255.18	268.92	275.96	289.82
2:20	———	———	———	———	———	———	———	———
2:50	192.04	204.77	215.58	233.56	270.00	285.11	292.36	306.39
3:00	———	———	———	———	———	———	———	———
3:20	194.85	207.77	218.62	236.96	277.00	292.72	299.74	314.14
3:40	———	———	———	———	———	———	———	———
4:00	194.81	207.73	219.69	238.63	282.27	295.28	302.25	315.55
4:20	———	———	———	———	———	———	———	———
4:40	196.00	208.32	220.00	238.67	284.64	298.82	306.11	320.07
5:00	———	———	———	———	———	———	———	———
5:20	196.04	208.32	220.77	239.15	284.75	298.61	305.86	319.89

RUN NUMBER 12*

heat input: 4000 BTU/hr

cooling water flow rate: 610 lb_m/hr

cooling water temperature
in: 63.5 °F
out: 70 °F

thermocouple readings in °F:

load ($lb \times 10^{-3}$)	thermocouple number							
	1	2	3	4	5	6	7	8
20	197.28	209.65	221.38	240.23	285.15	299.37	306.82	321.11
40	197.04	209.46	221.34	240.27	285.30	299.81	307.25	321.21
55	198.77	211.34	223.46	242.59	279.93	298.04	305.82	320.25

*Note: This run is a continuation of run number 11 with axial loading applied to the inner cylinder. The temperatures listed are steady state temperatures for the given load.

RUN NUMBER 13

heat input: 4130 BTU/hr

cooling water flow rate: 600 lb_m/hr

cooling water temperature
in: 62 °F
out: 70.5 °F

thermocouple readings in °F:

time	thermocouple number							
	1	2	3	4	5	6	7	8
0	81.35	—						→
:20	110.96	116.61	123.00	132.80	135.75	141.32	145.84	156.76
:40	146.04	154.32	162.84	176.20	181.48	191.24	197.48	210.35
1:00	165.52	175.92	186.00	201.44	213.85	225.50	232.50	246.04
1:20	176.76	187.96	198.58	215.15	236.67	249.81	256.81	270.81
1:40	184.48	195.44	206.12	223.04	251.26	268.00	275.21	289.36
2:00	188.56	200.50	212.00	229.59	263.04	281.15	288.28	302.61
2:20	190.80	203.08	214.81	233.22	271.81	291.07	298.46	312.82
2:40	193.19	205.23	216.93	235.96	274.37	293.43	300.71	314.14
3:00	193.88	206.31	218.19	237.08	277.14	297.78	305.14	319.71
3:20	194.72	207.08	218.96	238.30	281.48	303.57	310.89	325.71
3:40	196.38	208.68	220.35	239.33	289.39	308.78	315.86	330.32
4:00	198.65	211.42	223.23	242.15	294.04	311.04	318.69	332.61
4:20	198.77	211.15	222.85	241.78	297.57	312.36	318.59	331.55
4:40	200.81	213.31	225.12	244.11	299.22	314.82	321.18	335.71
5:00	201.28	213.96	225.73	244.74	302.21	317.61	324.68	339.17
5:20	199.73	212.85	224.81	244.81	305.06	320.36	327.34	341.90
5:40	201.04	214.15	226.44	246.42	306.64	321.71	328.50	343.07

RUN NUMBER 14*

Heat input: 4130 BTU/hr

cooling water flow rate: 600 lb_m/hr

cooling water temperature
in: 62 ^oF
out: 70.5 ^oF

thermocouple readings in ^oF:

load (lbs x10^{-3})	thermocouple number							
	1	2	3	4	5	6	7	8
20	200.23	213.34	225.77	245.85	307.11	322.93	329.96	344.83
40	200.23	212.81	224.74	244.92	306.28	322.71	329.31	344.31
57	200.92	213.84	225.84	245.15	305.50	321.21	328.64	343.55

*Note: This run is a continuation of run number 13 with axial loading applied to the inner cylinder. The temperatures listed are steady state temperatures for the given load.

XII. REFERENCES

1. Bibliography - Contact Thermal Conductance (to 1966), Bell Telephone Laboratories, No. 101, (Dec. 1966).

2. Kouwenhoven, W. B., Potter, J. H., "Thermal Resistance of Metal Contacts", J. Am Weld Soc, Vol 27, 515s-520s, (1948).

3. Brunot, A. W., Buckland, F. F., "Thermal Contact Resistance of Laminated and Machined Joints", Trans ASME, vol. 71, no.3, 253-257, (1949).

4. Weills, N. D., Ryder, E. A., "Thermal Resistance Measurements of Joints Formed Between Stationary Metal Surfaces", Trans ASME, Vol. 71, 259-267, (1949).

5. Fried, E., "Thermal Joint Conductance in a Vacuum", ASME publication, paper no. 63-AHGT-18, (1963).

6. Barzelay, M. E., Tong, K. N., Holloway, G. F., "Effect of Pressure on Thermal Conductance of Contact Joints", NACA TN 3295, (May 1955).

7. Minges, M. L., Thermal Contact Resistance, technical report AFML-TR-65-375, Vol. 1, (April 1966).

8. Veziroglu, T. N., Correlation of Thermal Contact

Conductance Experimental Results, NASA GRANT NGR 10-007-010-Sub 11, Interim Report No. 1, (Feb. 1967).

9. Faupel, J. H., Engineering Design, John Wiley and Sons, Inc., New York, (1964).

XIII. VITA

Roger Harold Stoudt, son of Mr. and Mrs. Roland Stoudt, was born on February 26, 1945, in Fullerton, Pennsylvania. He attended public schools in Orefield, Pennsylvania, where he graduated from Parkland High School in June of 1963. The following autumn he began studies at Lehigh University, Bethlehem, Pennsylvania in pursuit of a Bachelor of Science Degree in Mechanical Engineering. Mr. Stoudt graduated with high honors from Lehigh University in June, 1967.

In September of 1967, Mr. Stoudt returned to Lehigh University to study under an NDEA fellowship. He completed his program for a Master of Science Degree in Mechanical Engineering in September of 1968. He left Lehigh University to accept an engineering position in the Atomic Energy Divison of Babcock and Wilcox in Lynchburg, Virginia.

Mr. Stoudt is married to the former Joanne Stemrich of Allentown, Pennsylvania.